Criteria for the recognition of Archean calc-alkaline lamprophyres: examples from the Abitibi Subprovince

Lucie Mathieu[1]*, Émile Bouchard[1], Francis Guay[1], Alizée Liénard[1], Pierre Pilote[2], Jean Goutier[3]

[1]**L. Mathieu, E. Bouchard, F. Guay, A. Liénard.** Centre d'études sur les Ressources minérales (CERM) - Université du Québec à Chicoutimi, 555 boul. de l'Université, Chicoutimi, Canada, G7H 2B1

[2]**P. Pilote.** Ministère de l'Énergie et des Ressources Naturelles du Québec, 201, avenue du Président-Kennedy, Montréal, QC, Canada, H2X 3Y7

[3]**J. Goutier.** Ministère de l'Énergie et des Ressources Naturelles du Québec, 70, avenue Québec, Rouyn-Noranda, QC, Canada, J9X 6R1

***Corresponding author:** Lucie Mathieu (e-mail: Lucie1.Mathieu@uqac.ca; tel: 1-418-545-5011 ext. 2538)

Keywords: calc-alkaline lamprophyre (CAL), hydrothermal alteration, gold mineralisation, Abitibi, amphibole

Abstract

Lamprophyres are minor intrusions with atypical sources and crystallisation sequences. Among lamprophyres, the calc-alkaline type (CAL) on which this study focuses has the least distinctive chemistry and petrology. CAL correspond to small-volume mafic intrusions characterised by the early fractionation of amphibole and/or biotite. In the Archean Superior Province (Canada), CAL are temporally and spatially related to several gold deposits and may thus be relevant to mineral exploration. This study focuses on several altered and metamorphosed intrusions of the Abitibi and La Grande Subprovinces, which were designated lamprophyres based on field observations. Several criteria established from thin sections, whole-rock chemical analyses and SEM data are applied to the studied rocks in order to distinguish CAL from other types of magma. As a result, only one of the studied dykes has the morphology, chemistry, and petrology typical of CAL, while the other intrusions are either too altered to be classified or may correspond to metamorphosed and metasomatized gabbro and diorite. This study shows that thin sections and whole-rock chemical analyses are not always sufficient to unequivocally classify an altered and metamorphosed intrusion as a CAL. Also, intrusions as challenging to recognise as CAL should not be used by exploration geologists to prospect for orogenic gold deposits. Much remains to be done to document the distribution and volume represented by lamprophyres in Archean greenstone belts and to confirm their spatial dependence with gold deposits.

Introduction

Lamprophyres are small-volume intrusions with atypical chemistry. The term "lamprophyre facies" designates magmatic rocks with amphiboles and/or biotite phenocrysts and a feldspar-bearing matrix (Mitchell 1994, Le Maitre et al. 2002). The "facies" designation is descriptive and has no geodynamic implications (Mitchell 1994). The term "lamprophyre", on the other hand, designates small-volume volatile-enriched magmas produced by a small degree of deep partial melting of a metasomatized mantle (e.g. Wyman et al. 2006). These magmas are characterised by the early fractionation of amphibole and/or biotite, among other phases (Esperança and Holloway 1987, Ubide et al. 2014). Lamprophyres should be viewed as minor pulses of atypical magma. Lamprophyres are not portions of larger igneous complexes that crystallised in unusual conditions; i.e. they "are not simply textural variants of common plutonic or volcanic rocks" (cited from Streckeisen 1979, p. 333). The oldest known lamprophyre intrusions are Neoarchean; i.e. they are contemporaneous with the onset of alkaline magmatism and of modern plate tectonic dynamics (Wyman and Kerrich 1988, Kerrich and Wyman 1990).

This study focuses on calc-alkaline lamprophyres (CAL), also designated as shoshonitic or mafic lamprophyres, which are spatially and temporally related to gold deposits in Abitibi and in other Neoarchean greenstone belts (Rock and Groves 1988a, 1988b). The number of lamprophyres reported in the vicinity of gold deposits has led to "an adage among some gold prospectors that lamprophyres are good indicators of the presence of gold deposits" (cited from Boyle 1979, p. 250). This spatial and temporal relationship likely reflects the ability of crustal-scale structures to channel small-volumes of magma

and gold-bearing hydrothermal fluids (Kerrich 1986, Wyman and Kerrich 1989a, Kerrich and Wyman 1994, Dubé et al. 2004). A genetic link between gold deposits and lamprophyres was proposed in the 90s (Rock 1991, Groves et al. 1998). However, lamprophyres are a small volume of magma that would not contribute much gold and fluid to mineralising systems. Also, analyses of un-altered lamprophyres indicate that these magmas are not enriched in gold (Kerrich and Wyman 1994, Wyman et al. 1995). Nonetheless, lamprophyres may be more abundant near gold deposits (Hodgson and Troop 1988). They are generally closely temporally related to several gold mineralising events (e.g. Wyman and Kerrich 2010) and may be used as chrono-stratigraphic and structural markers. Lamprophyres may thus be useful when prospecting for gold. However, the recognition of lamprophyres modified by hydrothermal alteration and/or metamorphism is not straightforward. In this context, documenting the distribution of lamprophyres in greenstone belts is challenging. Also, are some varieties, like minette (i.e. the biotite- and orthoclase-dominated CAL variety), preferentially associated with gold deposits?

In this contribution, we perform detailed analyses on several small-scale intrusions of the Superior Province that display a lamprophyre facies. These rocks are classified as lamprophyres using a list of petrological and chemical criteria that can be applied in an exploration context. These criteria must thus be applicable to data such as field observations, whole rock chemical analyses, and petrological observations made with a standard microscope, which are accessible to exploration geologists. Additional criteria, discussed using a scanning electron microscope (SEM), are also presented.

Lamprophyre: criteria for their recognition

In this section, criteria for the recognition of CAL are listed (Table 1), and the applicability of these criteria on Archean lamprophyres will then be discussed. A first set of criteria can be applied in the field, where CAL: 1) are mafic to ultra-mafic shallow-level small-volume intrusions such as dykes, sills, and plugs (criterion Ia); 2) contain euhedral biotite and/or amphibole macrocrysts and a feldspar-dominated matrix (criterion Ib); and 3) may contain abundant xenoliths and ocelli (i.e. globular clusters of felsic minerals) (criterion Ic; Table 1) (Rock 1991).

The next set of criteria is chemical. Lamprophyres are mantle-derived magmas that are rarely differentiated (Rock 1987) and thus display elevated Mg# and Cr, Co, and Ni contents (criterion IIa). They also derive from a depleted mantle fertilised by metasomatism (Wyman and Kerrich 1993, Wyman et al. 2002, 2006) and are thus enriched in LILE and LREE (criterion IIb). Lamprophyres are produced by a small-degree of partial melting (about 5%; Bloomer et al. 1989, Gill and Whelan 1989) and tend to reflect the heterogeneous composition of their source (Wyman et al. 2006) (criterion IIc). Also, the CAL intrusions of the Superior Province display a relative depletion in the High Field Strength Elements (HFSE) Zr, Hf, Nb, Ta and Ti (Wyman et al. 1995), possibly because a phase retains these elements in the mantle (Arculus 1987, McCulloch and Gamble 1991) (criterion IId).

The last set of criteria is petrological. Lamprophyres are enriched in volatiles promoting the rapid rise of small volumes of magma in the crust (Sparks et al. 1977, Spera 1984). They may therefore contain CO_2- and H_2O-bearing phases such as magmatic carbonate, biotite, and/or amphibole (criterion IIIa); e.g. amphibole can only crystallise from H_2O-

enriched melt (Yoder and Tilley 1962, Bucholz et al. 2014). Lamprophyres are also characterised by the early fractionation of olivine, clinopyroxene, amphibole, and/or biotite (criterion IIIb). These minerals form at depth in a magma enriched in K_2O (to form biotite) and/or H_2O (to form amphibole) (Esperança and Holloway 1987, Murphy 2013, Bucholz et al. 2014, Ubide et al. 2014).

The main minerals observed in CAL may also display distinctive chemistry. Primary amphiboles (criterion IIIc; Table 1) are generally Mg-rich hastingsite, hornblende, and pargasite, and are less commonly edenite, kaersutite, richterite and tschermakite. These minerals display a magmatic zoning and are rimed by actinolite or hornblende (Allan and Carmichael 1984, Currie and Williams 1993, Lefèbvre et al. 2005, Plá Cid et al. 2007, Owen 2008). In his compilation, Rock (1991) gives a similar account by indicating that CAL generally contain the following titanian or potassian Ca-amphiboles: hastingsite, tschermakite, Mg-hornblende, and/or pargasite. Rock (1991) also indicates that the actinolite and actinolitic-hornblende reported in CAL are secondary amphiboles.

Primary biotite (criterion IIId), in lamprophyres, may be castellated, bent and/or kinked crystals, and is usually enriched in Ba, Ti, and F (Rock 1991). This mica is generally phlogopite with a clear magmatic zoning (Plá Cid et al. 2007). Secondary biotite, on the other hand, are coarse minerals that may replace amphibole and/or have the same chemistry as ground mass crystals (Lefèbvre et al. 2005).

Feldspar does not display characteristic chemistry. Indeed, feldspar have various Na/Ca ratios and a generally dominant anorthite (in kersantite and spessartite CAL varieties) or K-feldspar component (minette and vogesite) (Rock 1991). Also, in greenstone belts, the

pure albite observed in CAL is generally a metamorphic mineral of the greenschist facies (Perring et al. 1989).

Geological setting

The Superior Province of Canada contains several fault-bounded Subprovinces dominated by felsic complexes, greenstone, or metasedimentary rocks (Card 1990). This study focuses on lamprophyres observed in the La Grande (Eeyou Istchee Baie-James area) and Abitibi Subprovinces (Figure 1).

The Abitibi Subprovince is the largest and most economically significant greenstone belt of the Superior Province. Its geology and structure have been described by many authors (see Wyman and Kerrich 2009, and references therein). It contains Neoarchean volcanic, magmatic, and sedimentary rocks metamorphosed to low-grade subgreenschist, greenschist, and amphibolite facies (Jolly 1974, Faure 2015). Southern Abitibi is delimited by the Cadillac-Larder Lake fault, a structure known for its association with abundant gold mineralisation. The La Grande Subprovince is also a gold producer (Éléonore Mine). It consists of an assemblage of intrusive complexes and greenstone belts, and is older (ca. 3.45-2.57 Ga; Goutier et al. 2016) than the Abitibi Subprovince (ca. 2.79-2.64 Ga; Thurston et al. 2008, Goutier and Melançon 2010).

The Superior Province was assembled into a coherent craton by 2.60 Ga (Percival et al. 2006), and these successive accretionary events affect the tectonic evolution of individual Subprovinces. For example, in the Abitibi Subprovince, the construction or synvolcanic period is followed by a deformation phase, or syntectonic period, which comprises a succession of events such as shortening, regional metamorphism and sanukitoid

154 magmatism, followed by late transpression and orogenic gold mineralisation (Percival et
155 al. 2006).
156 In the Superior Province, lamprophyres are observed near the contacts between terranes
157 and may be genetically related to accretionary processes (Wyman and Kerrich 1989b,
158 1993, Card 1990). Many lamprophyres have been recognised in Abitibi (Figure 1). There,
159 they correspond to syntectonic magmatic activity: lamprophyres formed at about 2710
160 Ma in the north of the Subprovince to 2670 Ma in the south, and are coeval with orogenic
161 gold deposits (Kerrich and Wyman 1994). They are also spatially and temporally related
162 to syntectonic magmatic manifestations such as syenite, monzonite, monzodiorite, and
163 shoshonite (Sims and Mudrey 1972, Schulz et al. 1979, McNeil and Kerrich 1986,
164 Wyman and Kerrich 1989a, Wesley McCall et al. 1990, Carter 1992). In the La Grande
165 Subprovince however, temporal associations between lamprophyres, other intrusions and
166 deformation are less documented.
167 The small-volume intrusions with lamprophyre facies selected for this study are located
168 in the La Grande Subprovince and near the Cadillac-Larder Lake fault, in southern
169 Abitibi (Figure 1; Table 2). These intrusions are spatially related to deformation zones,
170 gold showings, and/or minor felsic intrusions; they are metamorphosed and may have
171 been hydrothermally altered. The selected samples offer a diverse view of the lithologies
172 typically mapped as lamprophyres in the Superior Province.
173 ***Lamp_FG samples*** – These samples were collected by F. Guay as part of his Master
174 study of the Malartic Lakeshore outcrop located about 6 km north of the Cadillac-Larder
175 Lake fault. It exposes the Rivière Héva fault zone (Pilote 2013, 2014), which separates
176 the following volcanic units: 1) mafic volcanic units in the south that are part of the

177 2708±2 Ma Dubuisson Formation (Malartic Group; Pilote 2007); and 2) felsic
178 volcaniclastic units in the north that are part of the 2702±1 Ma Héva Formation (Malartic
179 Group; Davis 1998). An unexposed tonalite intrusion is known from geophysical and
180 drilling data (Bousquet and Carrier 2009a, 2009b). The outcrop contains a gold showing
181 (Lac Malartic showing, property of Khalkos Exploration Inc.) consisting of deformed
182 quartz veins. Alteration (i.e. carbonatisation, epidotisation, and K-metasomatism) formed
183 biotite in the mafic units (Guay et al. 2015). The quartz-veins are cross-cut by many thin
184 dykes (< 1 m thick) with a lamprophyre facies. The samples studied here are from biotite-
185 (FG-02) and amphibole- (FG-07) enriched dykes (Figure 2-a).
186 ***Lamp_AL samples*** **–** These samples have been collected by A. Liénard as part of her
187 Master study of an outcrop previously studied by Scott et al. (2002). The sampled area is
188 located 1 km east of the Sigma gold mine (see Robert and Brown 1986, and references
189 therein) and a few kilometers NE of the Lamaque mine. The outcrop exposes felsic-
190 intermediate volcanic rocks of the Val-d'Or Formation (see Taner and Trudel 1991,
191 Pilote 2013, 2014, and references therein), dykes with various compositions, as well as E-
192 W-striking shear zones and quartz-tourmaline veins. The Lamp_AL samples come from a
193 lithology with a lamprophyre facies and a poorly defined geometry (Scott et al. 2002),
194 which may correspond to the xenolith-bearing margin of a possibly larger plug-shaped
195 intrusion. The xenoliths are <5 cm to up to meter-long fragments of thin to coarse grained
196 mafic to felsic crustal rocks, and represent about 5 vol% of the exposed lithology (Figure
197 2-b).

198 ***Lamp_Carb sample*** **–** This poorly exposed intrusion has been sampled by the MERN
199 (Ministère de l'Énergie et des Ressources Naturelles, Québec) in the Blake River Group.
200 It has been identified as a strongly carbonatized mafic lamprophyre.
201 ***Lamp_BJ samples*** **–** These 50 cm to a few meters thick dykes of the Baie-James area
202 (Figure 1) have been sampled by the MERN and studied by Côté-Vertefeuille (2016).
203 They are mostly hosted by basalts and tonalites, and are not spatially related to gold
204 showings.
205

206 # Methodology

207 Whole rock chemical analyses and standard thin sections are available for the bulk of the
208 studied samples. Chemical analyses (Table 2) have been performed according to MERN
209 standards. Rigorous quality assurance – quality control (QA–QC) procedures were
210 maintained, including the use of blanks, standards, and duplicates, to obtain precise and
211 accurate results. The samples were decomposed by lithium metaborate or tetraborate
212 fusion and were analyzed at Activation laboratories Ltd. (Actlabs) by ICP-OES and ICP-
213 MS for major and trace elements, respectively. The detection limits are 0.01 wt% for
214 major elements, and vary from 0.1 to 1 ppm for the trace elements reported in Table 2
215 (for details, see actlabs.com).
216 Petrological observations are performed with a conventional microscope. For the
217 Lamp_FG samples, backscattered electron images and chemical maps (major elements),
218 as well as point semi-quantitative analyses of various minerals (beam diameter of 1.7
219 microns) were acquired with a SEM (Zeiss EVO-MA15 HD 2013) located in Chicoutimi
220 (IOS services géoscientifiques Inc.). The FeO/Fe_2O_3 ratio and volatile content of the

analysed minerals could not be measured. Structural formulas are nonetheless calculated with total iron as Fe_2O_3 for epidote, and on an 8, 12.5, 11, and 23 oxygens basis for feldspar, epidote, biotite, and amphibole, respectively. For biotite, calculations are performed with a modelled FeO/Fe_2O_3 ratio, assuming that site A is filled with K+Na+Ca and that the mineral contains 2H apfu. The structural formula of amphiboles correspond to the mean of the estimates made assuming maximum and minimum values for the FeO/Fe_2O_3 ratio, following the procedure recommended by Leake et al. (1997).

This study also considers chemical data of 121 abitibian CAL compiled from the literature (Watson 1957, Goldie 1979, McNeil and Kerrich 1986, Schandl et al. 1989, Sutcliffe et al. 1990, Barrie and Shirey 1991, Bourne and Bossé 1991, Wyman and Kerrich 1993, Camiré et al. 1993, Morin et al. 1993, Rowins et al. 1993, Wyman et al. 1995, 2006, Hattori et al. 1996, Lefèbvre et al. 2005). In addition, the chemistry of non-lamprophyre magmatic rocks from the Superior Province has been considered using the Georoc web database (Sarbas and Nohl 2008, GEOROC 2011), from which analyses with major and trace elements available were downloaded (n=1679 samples). The given names of these rocks were then simplified as follows: 1) komatiite (includes also pyroxene- and olivine-cumulates); 2) ferropicrite; 3) basalt (stands for gabbro, tholeiite, hawaiite, boninite); 4) andesite (includes also diorite); 5) dacite (includes also rhyodacite); 6) rhyolite (includes also granite); and 7) other (regroups mugearite, shoshonite, syenite, tephrite, carbonatite, trachyte, trachyandesite, absarokite, tristanite, tonalite, trondhjemite, and adakite). The Georoc data were supplemented using 307 data from Beakhouse (2011), which are designated pretectonic, syntectonic, latetectonic and minor intrusions.

Results

Whole rock composition

Compared to the 1590 CAL samples compiled by Rock (1991), the studied samples contain less TiO_2 and samples ML-05-056 and 98-FF-11108-A1 contain less Al_2O_3 than the average CAL (Table 2). Also, Rock (1991) indicates that most CAL are potassic rocks ($K_2O > Na_2O$), while only Lamp_Carb is potassic, FG-07 is sodic ($Na_2O - 4 > K_2O$), and the other samples have compositions intermediate between potassic and sodic rocks. The alkali and silica content of CAL is however extremely variable and most of the studied samples fall within the CAL field defined by Rock (1987) on the TAS diagram (Figure 3). Note that these preliminary remarks on major elements do not consider possible alteration-related modifications.

The trace elements content of the studied dykes falls within the lower range of variations observed for abitibian CAL (Figure 4-a). These dykes are enriched in compatible (e.g. Cr generally > 300 ppm) and incompatible (e.g. La = 20-35 ppm) elements (Table 2). With the exception of the 98-FF-11108-A1 and 11-JG-1197-A samples, they display relatively pronounced Zr and Hf negative anomalies. The studied intrusions also display the Ta-Nb-Ti (TNT) negative anomaly observed in most Abitibi magmas (e.g. Beakhouse 2011) and in CAL around the World (Rock 1991). The FG-07 sample is the most fractionated (La/Y = 3.3), while the other samples display a flatter spectrum due to Heavy Rare Earth Elements (HREE)-enrichment (La/Y = 1 to 1.5) (Table 2). Moreover, the studied dykes have incompatible elements-content (e.g. La; Figure 4-a) intermediate between those of calc-alkaline and alkaline magmas (Figure 4-b).

To further compare these samples to the Georoc dataset, a principal component analysis (PCA) has been performed on the following parameters: 1) Th_ABS = log(Th*) (with * designating an element normalised to the primitive mantle of Hofmann 1988); 2) Yb_ABS = log(Yb*); 3) ZrHf_Ano = (Zr*+Hf*)/(Nd*+Sm*); and 4) Slope, which quantifies trace element fractionation. The Slope parameter is the slope of linear regressions going through [x, y] points expressed as [log(A*), B], with A = [Th, La, Ce, Pr, Nd, Sm, Gd, Tb, Dy, Ho, Y, Er, Tm, Yb] and B = [19, 16, 15, 14, 13, 10, 8, 7, 6, 5, 4, 3, 2, 1]. The PCA is a coordinate transformation method that can be used to combine variables. In PCA, data are represented in the *m* dimensional space as an ellipsoidal cloud of *n* points whose first, second and third longest axes correspond respectively to the first, second, and third principal component (PC1, PC2 and PC3), and so on. By considering only PC1 and PC2 (Figure 5), the dimensionality of the data is reduced from *m* to 2 variables. In our case, *m* = 4 variables (i.e. Th_ABS, Yb_ABS, ZrHf_Ano, Slope), *n* = 1189 data (i.e. compiled data with at least Th, Yb, Zr, Hf, Nb and Sm analysed), and a mean centre transformation was performed to facilitate the combination of the variables.

The results of the PCA (Figure 5; Table 3) show that, compared to other types of magmas, lamprophyres are characterised by intermediate to elevated Slope parameter (i.e. pronounced fractionation), pronounced Zr and Hf negative anomalies (ZrHf_Ano parameter), as well as elevated Th and relatively low Yb contents (Th_ABS and Yb_ABS parameters). Examining Figure 5, we observe that most lamprophyres form a cluster, but they can be mistaken for rocks of the “minor intrusions”, “latetectonic”, and “other” categories (i.e. mostly alkaline and calc-alkaline pre- to late-tectonic intrusions; see Pie diagrams of Figure 5). Additional tests show that, compared to the other rocks of the

289 Superior Province, the Nb and Ta negative anomalies of lamprophyres are particularly
290 pronounced, their Ti anomaly is within the range of those observed in other rocks, and
291 their Cr content is elevated but not discriminant.
292
293 **Minerals and textures**
294 Observations made with a conventional microscope confirm that, in the Lamp_Carb
295 sample (ML-05-056), carbonates (Table 4) and carbonate-filled vesicles (Figure 6-e, f)
296 are abundant and that magmatic textures are not preserved due to intense carbonatisation.
297 Among the Lamp_BJ samples, sample 98-FF-11108-A1 is dominated by actinolite
298 (Figure 6-a), while the other samples contain mostly green hornblende, biotite, and
299 feldspar (Table 4; Figure 6). The matrix is dominated by locally sericitised albite and
300 microcline, and ±quartz. The clusters of amphibole and biotite megacrysts observed in
301 sample 99-MH-4589 may correspond to xenoliths (Table 5). Magmatic textures are
302 poorly preserved in the Lamp_BJ samples, possibly as a consequence of metamorphism.
303 The Lamp_AL samples are dominated by about 0.5 to 2 mm long macrocrysts of biotite
304 that growth at the expense of amphibole (about 3/4 hornblende and 1/4 actinolite) (Figure
305 7-e, f; Tables 4 and 5). The matrix consists of ~0.5 mm long moderately to strongly
306 sericitised feldspar, and minor amount of carbonate and epidote. The most silica-enriched
307 samples contain interstitial quartz. Magmatic minerals and textures are poorly preserved
308 in these altered and metamorphosed rocks.
309 The Lamp_FG samples are also dominated by amphibole, biotite, and a feldspar-enriched
310 and quartz-bearing (FG-02 sample only) matrix, and contain epidote, titanite, and apatite
311 (Table 4 and 5). The amphiboles of the FG-07 sample are euhedral, and both the lozenge-

312 shaped and elongated sections are zoned with a brown core and a green rim (Figure 7-a,
313 b); a zoning often reported in lamprophyres (Watson 1957, Rock 1991). This zonation is
314 not observed in sample FG-02. This sample also contains the largest amount of biotite
315 and epidote that growth at the expense of amphibole and other minerals (Figure 7-c, d).
316
317 **Minerals of the FG-02 and FG-07 samples**
318 This section presents additional textural and chemical data obtained with a SEM for
319 samples FG-02 and FG-07. The backscattered electron SEM images reveal that the
320 amphiboles of the FG-07 sample have a complex structure (Figure 8) made of: 1) zone A
321 designating the core; 2) zone B designating the brightest backscatter intermediate rim;
322 and 3) zone C designating the outer darkest backscatter rim of the amphibole. Zones A,
323 C, and ±B are well developed in the largest, lozenge-shaped, macrocrysts (Figure 8-a, b,
324 c), while the elongated crystals are mostly made of zones B and C (Figure 8-d, e, f).
325 Zones A and B have gradational contacts with an Mg-rich core (zone A) and a denser Fe-
326 enriched rim containing biotite inclusions (zone B) (Figure 9-a, b). Zones A and B may
327 correspond to a normally-zoned truncated lozenge-shaped hornblende (Figure 8-b), while
328 zone C is likely an actinolite (Figure 8-a, b). The contact between zone C and zones A-B
329 is sharp and irregular (Figure 8-b).
330 By contrast, the amphiboles of the FG-02 sample are poorly zoned and mostly consist of
331 the darkest backscatter zone C (Figure 10). They also display a lighter backscatter core
332 (i.e. zone B) that has gradational and irregular contacts with zone C (Figure 10-a). In
333 some amphiboles, zone B forms minor linear features within zone C (Figure 10-e, f).
334 Biotites, in the FG-02 sample, are large un-zoned minerals that, together with epidote,

grew at the expense of amphibole (Figure 10). A part of these minerals is associated with titanite likely accommodating the TiO_2 released by the destabilised amphibole. Matrix minerals are feldspar (FG-07) or about 1/3 quartz and 2/3 feldspar (FG-02).

Alteration in the FG-02 sample is uniformly distributed. It is mostly characterised by abundant epidote and by biotite locally retrograded to chlorite. The FG-07 sample contains minor epidote and clusters, located in the central part of the dyke, that are zoned as follows: 1) amphibole and epidote assemblage in the outer part; and 2) a core mostly made of amphibole, calcite, and titanite (Figure 9-c, d).

According to semi-quantitative chemical analyses, zones A and B of both Lamp_FG samples have the chemical composition of tschermakite to Mg-hornblende amphiboles (Figure 11). The Mg# of zone A amphiboles is generally higher than in zone B. Zone C minerals are actinolite to ±Mg-hornblende. These amphiboles have Al-rich and Si-poor cores. In addition, zones A and B are Na-rich (0.45-0.5 Na apfu), Ti- and K-bearing (about 0.15 apfu each) amphiboles, while zone C is almost Na-K-Ti-barren (Table 6). The micas are mostly biotite to ±phlogopite (Figure 12). The feldspars are pure albite (Ab_{97-99}). The epidotes have the general formula $Ca_2Al_{2.5}Fe_{0.5}Si_3O_{12}(OH)$ (sample FG-07) and $Ca_2Al_{2.2}Fe_{0.8}Si_3O_{12}(OH)$ (sample FG-02).

Discussion

The studied samples have been designated lamprophyres based on field observations. In this section, the petrological and chemical characteristics of these samples will be discussed and compared to the list of criteria presented in the “definition” section.

Criterion I – lamprophyre facies (field observations)

The studied rocks are mafic shallow-level small-volume intrusions with abundant euhedral biotite and amphibole macrocrysts: they have a lamprophyre facies and fit criteria Ia and Ib (Table 7). The only exception is the Lamp_Carb sample, in which carbonatisation destabilised the amphibole macrocrysts. Even if the Lamp_AL sample, and possibly the 99-MH-4589 sample, contain some crustal xenoliths (Figure 2-b), the studied rocks lack the abundant xenoliths and ocelli often observed in lamprophyres (e.g. Rock 1991). This last characteristic is judged non-critical and, according to criterion I, the bulk of the studied rocks could be CAL.

However, in Abitibi, many syn- to late-tectonic magmatic intrusions contain amphibole and/or biotite (e.g. Leduc 1980, Sutcliffe et al. 1990, 1993) which either pseudomorph pyroxene or correspond to primary minerals. The recognition of a lamprophyre facies is thus insufficient to classify an intrusion as a lamprophyre and additional evidence needs to be presented; e.g. presence of early crystallised magmatic amphibole and biotite (phenocrysts) with particular chemistry (see below).

Criterion II – whole-rock chemistry

The studied rocks have variable major elements contents that fall within the ranges of Na, K, and Si variations known for CAL (Figure 3). Only sample 98-FF-11108-A1 may not be a lamprophyre because it is alkali-depleted and Al_2O_3-poor. Compared to the samples compiled by Rock (1991), the FG samples have compositions closest to those of speassartite; i.e. the K_2O-poorest, amphibole and plagioclase-bearing, CAL variety. The

major elements content of lamprophyres, however, is too variable (Rock 1991) to be used to classify these intrusions.

Concerning trace elements, with the exception of the FG-02 sample that may be the most differentiated, the intrusions are Cr-, Co-, and Ni-enriched rocks with elevated Mg#. These rocks likely have a mantle source and fit criterion IIa (Table 7). The studied rocks are also enriched in incompatible elements (criterion IIb) and have LILE and LREE contents intermediate between those of Abitibi felsic calc-alkaline and alkaline intrusions (Figure 4). Such intermediate compositions are probably a distinctive characteristic of CAL.

The composition of the plug outcrop located east of Val-d'Or city, for which the largest number of samples are available (Lamp_AL), is heterogeneous due to fractional crystallisation (see alignment of samples on the TAS diagram; Figure 3) and/or to assimilation (see xenoliths; Figure 2-b) processes. The other intrusions have not been sufficiently sampled to enable a discussion on their possible heterogeneous composition and to conclude on the degree of partial melting (see criterion IIc). However, the LILE, LREE, and HREE contents of the studied rocks fall within the range of the trace elements contents of the other lamprophyres observed in Abitibi (Figure 4-a): the studied rocks probably have similar source and production conditions.

The studied samples display Zr and Hf negative anomalies (criterion IId), which are observed in other intrusions in Abitibi (e.g. Beattie Syenite; Mathieu 2016). The samples also display the Ti, Ta, and Nb negative anomalies observed in most Abitibi magmas, possibly because these elements are retained in the mantle by titanite (Thompson et al. 1983, 1984, Venturelli et al. 1984, Rowins et al. 1993) or other processes (Pearce 1983).

The HFSE depletion is not a distinctive characteristic of CAL. Their variable enrichment in HREE and relatively elevated Th content are also within the range of those observed in other rocks (Figure 4-b).

In conclusion, the trace elements content of CAL appears variable (Figure 4-a) and not distinctive. This is confirmed by the PCA analysis, which is unable to distinguish CAL from the other products of syntectonic magmatic activity in Abitibi (Figure 5). In summary, the distinctive characteristics of CAL are an unusual fractional crystallisation sequence triggered by abnormal water contents (i.e. early fractionation of amphibole) and a rapid rise in the crust of small volumes of magma. The identification of CAL thus mostly relies on petrological criteria.

Criterion III – petrology

The studied samples are metamorphic rocks that may have been altered and have not retained primary carbonate, olivine, or clinopyroxene (criterion IIIa). To classify these rocks as CAL, the magmatic origin of amphibole and/or biotite needs to be confirmed.

The ML-05-056 sample has been too intensely altered to enable further petrological investigations. The metamorphosed Lamp_BJ samples do not retain magmatic textures. However, the protolith of the actinolite-dominated 98-FF-11108-A1 sample is unlikely to have contained alkali-bearing amphiboles. This sample is the most depleted in alkali and incompatible elements and is unlikely to be a lamprophyre. The biotite of the other Lamp_BJ samples and of the Lamp_AL samples does not display any of the textural characteristics of the primary biotite commonly observed in CAL (Rock 1991). In addition, these biotites are unlikely to be alteration minerals, as the Lamp_BJ and

Lamp_AL samples do not appear to be altered. A similar remark can be made on the amphiboles of these samples. In the absence of primary minerals and without access to the chemical composition of amphibole, the nature and composition of the magmatic phases replaced by secondary biotite and amphibole cannot be established. The Lamp_BJ and Lamp_AL samples cannot be unequivocally classified as CAL.

The Lamp_FG samples are different, because they retain magmatic textures. The zoned euhedral amphiboles observed in these samples are tschermakite to Mg-hornblende (zones A and B) and Mg-hornblende to actinolite (zone C). In Abitibi, the amphiboles observed in diorite, syenite, tonalite and mozonite are edenite, pargasite, hornblende and actinolite (Sutcliffe et al., 1990), while these observed in CAL also include tschermakite and Mg-hornblende (Rock, 1991). Zones A and B amphiboles have thus the typical chemistry of CAL primary amphiboles, whereas zone C is likely secondary. Also, primary amphiboles have been reported from relatively fresh intrusions as well as altered and/or metamorphosed lamprophyres (Perring et al. 1989, Camiré et al. 1993, Currie and Williams 1993, Williams 2002). Observing relics of primary amphiboles in a CAL metamorphosed to greenschist grade, like the FG-07 sample, is thus not without precedent.

The primary amphibole of sample FG-07 is normally-zoned (i.e. Mg-core and Fe-richer rim). Zone B also contains biotite inclusions, which either originate from a magma that crystallised amphibole followed by amphibole and ±biotite, or from the nucleation of biotite along the crystal-liquid interface before the whole magma reached the point of biotite-saturation (Green and Watson 1982). Because FG-07 has been altered and because the amphibole and its inclusions are likely the only magmatic relic minerals, it is not

449 possible to determine whether biotite was a near-liquidus phase. Also, lamprophyres are
450 generally enriched in foreign material (xenocrysts and xenoliths) (Rock 1991). In the FG-
451 07 sample, secondary phases prevent any comparison between the chemistry of the
452 macrocryts and that of the matrix minerals. It thus remains uncertain whether zones A
453 and B amphiboles are phenocrysts, antecrysts, or xenocrysts.
454 Zones C amphibole has a texture contrasting with those of zones A and B amphiboles. In
455 the FG-07 sample, zone C amphibole is thinly zoned, inclusion barren, and forms an
456 overgrowth around, and locally within, the magmatic amphibole. Zone C amphibole
457 probably originates from the alteration- and/or metamorphism-related destabilisation of
458 magmatic amphiboles. By analogy, most of the amphiboles of the FG-02 sample are
459 secondary. The feldspar is pure albite and is likely a secondary greenschist facies
460 mineral.
461 Biotite, in the Lamp_FG samples, forms un-zoned macrocrysts with the composition of
462 Mg-rich biotite. The biotite in sample FG-02 replaces amphibole and does not have the
463 chemistry of typical primary CAL biotite. Given that the host basalt developed
464 hydrothermal biotite as a result of K-metasomatism, it cannot be excluded that the
465 abundant biotite observed in FG-02 is secondary and possibly related to the same
466 alteration event. The coarse biotite observed in sample FG-07 is also secondary and
467 formed from the breakdown of amphibole (Figure 7-a, b), but biotite is not abundant in
468 FG-07 indicating that K-metasomatism is minor to absent in this dyke. Finally, epidote,
469 calcite, and titanite are likely alteration products that will be discussed in the next section.
470 In conclusion, the FG-07 sample retains primary amphiboles typical of those generally
471 reported in CAL and is probably a slightly altered CAL. The FG-02 sample could be a

lamprophyre according to its chemistry and to the similarities between its petrology and the petrology of FG-07. However, this sample does not retain enough primary minerals to be unequivocally classified as a CAL.

Implications for the recognition of hydrothermal alteration

Besides having a spatial relationship with gold mineralisation, lamprophyres are chrono-stratigraphic markers temporally related to many deposits (Kerrich 1986, Rock and Groves 1988b, Kerrich and Wyman 1994, Dubé et al. 2004). As such, estimating alteration in these intrusions could be useful to our understanding of mineralising systems. This is not an easy exercise with CAL, as will be demonstrated using the Lamp_FG samples.

The mineralogical modifications observed in sample FG-07 concern amphibole (zone C) and feldspar. Gains and losses of mobile elements are not required to turn magmatic plagioclase into an assemblage of epidote and albite, and the iron measured in the epidote may originate from the amphibole. The formation of zone C actinolite from zone A tschermakitic hornblende requires loss of Al and gain of Si, which may have been exchanged through reaction with feldspar. Alternatively, Si and Al may come from zone B, which is Si-poorer and Al-richer than zone A. Also, the Na of zone A amphibole may have been transferred to feldspar, or may have been lost. In summary, H_2O-gain and mineralogical changes are sufficient to form zone C amphibole, albite and epidote, while K-gain is necessary to form the coarse biotites observed in the FG-07 sample.

Alteration in sample FG-07 is locally more intense, where the amphibole-albite assemblage is progressively turned into amphibole-epidote and amphibole-calcite-titanite

assemblages (Figure 9-c, d). To form these assemblages, carbonatation, possibly with a gain in Ca (formation of calcite, etc.) and a loss in Na (destruction of albite), are required. Note that the zoned amphibole (zones A and B) seems particularly resistant to such alteration, whereas feldspar has been completely destabilised.

In conclusion, only hydration, locally carbonatisation, and possibly minor Na-loss and local Ca-gain (and K-gain?) are required to form the assemblages observed in sample FG-07. In this sample, mineralogical modifications are a consequence of: 1) self-alteration of a volatile-enriched intrusion; 2) carbonatisation by an external fluid; and/or 3) metamorphism-related hydration. These alteration considerations indicate that zone A may be a pristine magmatic amphibole, while zone B may have been slightly modified and all the other phases should be regarded as secondary. They also indicate that the gain or loss of major elements is limited, and that the whole rock chemical composition of the FG-07 dyke might be relatively representative of its pre-alteration composition.

In sample FG-02, amphibole is dominated by zone C; only relics of zone B are observed. This observation, as well as the large amount of epidote observed in this rock, indicates that FG-02 has been more intensely altered than FG-07. By analogy to the FG-07 sample, hydration and re-organisation of elements may be responsible for the formation of epidote, pure albite, and zone C amphibole in the FG-02 dyke. However, FG-02 is distinct in that most of zone C amphibole is replaced by biotite. This requires addition of K_2O that either diffused from feldspar and primary amphibole or, more likely, was added by a hydrothermal fluid. Other biotite elements (i.e. MgO, FeO, Al_2O_3, and SiO_2) may have been inherited from amphibole. However, for a constant amount of the immobile element Al_2O_3, biotite cannot accommodate the same amount of SiO_2 as actinolite. The

quartz observed in the FG-02 dyke is either magmatic or at least partly a side effect of the formation of biotite at the expanse of amphibole.

In conclusion, alteration in sample FG-02 is mostly characterised by K-gain, which is an important alteration effect recorded proximal to several orogenic (Groves et al. 1998 and references therein) and other gold systems.

Implication for the classification of CAL

As discussed above, sample 98-FF-11108-A1 is not a lamprophyre according to its petrology and chemistry. This mafic intrusion is more likely a calc-alkaline gabbro. The FG-07 sample can be classified as a lamprophyre as it retains magmatic biotite and Na-bearing amphibole, and displays a typical lamprophyre morphology (i.e. thin late dyke; Figure 2-a). The FG-02 sample could be an altered equivalent of the FG-07 dyke, but it is also more differentiated (e.g. lower Cr-content and quartz observed in thin section) and most of its mafic macrocysts (i.e. biotites) are alteration products. It cannot be excluded that this sample comes from a monzonite or diorite dyke, depending on the intensity of K-metasomatism.

Concerning the other samples, the Lamp_Carb intrusion has been too intensely carbonatized to be classified. The Lamp_BJ samples do not retain magmatic phases, due to metamorphism. As their geological context is different (La Grande Subprovince) and less documented, potential alteration and the relationship to other magmatic complexes are not clear. These samples cannot be clearly classified as lamprophyres.

The Lamp_AL samples have also been modified by metamorphism and ±alteration, and their geological context is well constrained (Abitibi Subprovince). A few kilometres west

and south of these samples, the Lamaque gold deposit is spatially associated with about 6 irregular intrusive bodies (plugs) of tonalite, diorite, and granodiorite with tholeiitic and calc-alkaline affinities (Daigneault et al. 1983, Grant 1986, Robert and Brown 1986). The Lamaque deposit is mostly contained in a zoned plug ("main chimney") consisting of a biotite-enriched and orthopyroxene-, amphibole-, oligoclase- and ±quartz-bearing diorite outer zone, a biotite-bearing tonalite (Daigneault et al. 1983) or granodiorite (Wilson 1936, Burrows et al. 1993) core, and an intermediate zone of quartz-diorite (Wilson 1936). The chemical composition of these diorites is comparable to this of the Lamp_AL samples (Figure 13). Chemistry has however proved unable to discriminate lamprophyres from diorite and other rocks (Figure 5).

A comparison between the Lamp_AL samples and the plugs observed in their vicinity will necessitate dedicated studies that are beyond the scope of this paper. We conclude that, while the Lamp_AL samples share common characteristics with lamprophyres (i.e. chemistry, general field characteristics), they also resemble nearby plugs (i.e. chemistry, possibly petrology). It cannot be excluded that they correspond to the contaminated margin (Figure 2-b) of a larger and possibly plug-shaped intrusion formed by the same intrusive event that produced the nearby plugs.

The challenges associated with the classification of CAL emphasised by this study also have consequences for the known distribution of mafic lamprophyres in Archean cratons. In Abitibi, for example, several CAL have been studied, whereas others have only been recognised in the field (lamprophyre facies) (Figure 14). According to the available data (Figure 14), it appears that lamprophyres intrude many types of rocks and occur in various structural settings both close to and far from major faults. They emplace prior and

after gold mineralisation, depending on the area, and form during the syntectonic period, but the temporal relationship between these intrusions and the tectonic evolution of the Subprovince remains to be documented in details. Only a systematic investigation of these intrusions enables a distinction between CAL and non-lamprophyric intrusions, providing answers to the questions: Are lamprophyres related to major deformation corridors and are they more abundant in the vicinity of orogenic gold deposits?

Conclusions

Lamprophyres in general, and CAL in particular, have been reported in various locations in the Superior Province of Canada (Figure 1). This study shows that the recognition of CAL is not straightforward: amongst the samples with a lamprophyre facies studied here, one is clearly a lamprophyre (FG-07), one is a gabbro or a related mafic cumulate (98-FF-11108-A1), one is a monzonite or a diorite (FG-02), another is either a lamprophyre or a contaminated diorite (Lamp_AL samples), whereas the others have been too intensely altered and/or metamorphosed to be unequivocally classified as CAL. Thus, based on this study, the distribution of CAL in the Superior Province is not clear.

This contribution also shows that the recognition of lamprophyres using analytical methods commonly accessible in an exploration context (i.e. field description, whole-rock chemical analyses, and conventional microscope) is challenging. Using the SEM instrument, which is relatively inexpensive, accessible, and requires limited sample preparation, the classification of unusual intrusions and the documentation of alteration is easier, as was demonstrated using the Lamp_FG samples. However, we conclude that CAL should not be used by exploration geologists to prospect for gold deposits, since

field recognition of CAL is challenging. In addition, available data are not sufficient to confirm that lamprophyres are more abundant near orogenic gold deposits.

Acknowledgments

Special thanks are addressed to editor Ali Polat, associate editor Brendan Murphy, and to Georgia Pe-Piper and John D. Greenough, who greatly helped to improve this contribution. The Master studies of F. Guay and A. Liénard are supported by the Ministère de l'Énergie et des Ressources Naturelles of Québec. The SEM analyses were supported by the Consorem Research Group (Consortium de recherche en exploration minérale), and thanks are addressed to Réjean Girard and Valérie Lecomte (IOS services géoscientifiques Inc.). This study was performed on behalf of the Consorem Research Group, which is supported by Canada Economic Development, the MERN, the Société du Plan Nord, and company members of Consorem. Warm thanks are also addressed to Réal Daigneault, Jérôme Lavoie, Sylvain Trépanier, Stéphane Faure, Silvain Rafini, and Ludovic Bigot for constructive discussions on this project. This is contribution number MERN 8449 – 2017-2018 – 05 of the Ministère de l'Énergie et des Ressources Naturelles.

References

Allan, J.F., and Carmichael, I.S.E. 1984. Lamprophyric lavas in the Colima graben, SW Mexico. Contributions to Mineralogy and Petrology, **88**: 203–216.

Arculus, R.J. 1987. The significance of source versus process in the tectonic controls of

magma genesis. Journal of Volcanology and Geothermal Research, **32**: 1–12.

Barber, R. 1996. Lac Mcvittie Joint Venture. O.M.I.P. report.

Barrie, C.T. 1990. U–Pb garnet and titanite age for the Bristol Township lamprophyre suite, western Abitibi Subprovince, Canada. Canadian Journal of Earth Sciences, **27**: 1451–1456.

Barrie, C.T., and Shirey, S.B. 1991. Nd-and Sr-isotope systematics for the Kamiskotia–Montcalm area: implications for the formation of late Archean crust in the western Abitibi Subprovince, Canada. Canadian Journal of Earth Sciences, **28**: 58–76.

Beakhouse, G.P. 2011. The Abitibi Subprovince plutonic record: Tectonic and metallogenic implications. Ontario Geological Survey, Open File, **6268**: 1–161.

Bédard, L.P., and Chown, E.H. 1992. The Dolodau dykes, Canada: an example of an Archean carbonatite. Mineralogy and Petrology, **46**: 109–121.

Bleeker, W., and Parrish, R.R. 1996. Stratigraphy and U–Pb zircon geochronology of Kidd Creek: implications for the formation of giant volcanogenic massive sulphide deposits and the tectonic history of the Abitibi greenstone belt. Canadian Journal of Earth Sciences, **33**: 1213–1231.

Bloomer, S.H., Stern, R.J., Fisk, E., and Geschwind, C.H. 1989. Shoshonitic volcanism in the northern Mariana arc, 1, Mineralogic and major and trace element characteristics. Journal of Geophysical Research: Solid Earth, **94**: 4469–4496.

Bourne, J.H., and Bossé, J. 1991. Geochemistry of ultramafic and calc-alkaline lamprophyres from the Lac Shortt area, Quebec. Mineralogy and Petrology, **45**: 85–103.

Bousquet, D., and Carrier, A. 2009a. Programme de forage 2008 sur l'indice aurifère

« RLM », propriété Malartic Lake Shore, Corporation Minière Golden Share / 2008 drilling program on the gold showing « RLM », Malartic Lake Shore property, Mining Corporation Golden Share. MERN report GM-64938.

Bousquet, D., and Carrier, A. 2009b. Programme de forage 2009 sur l'indice aurifère « RLM », propriété Malartic Lake Shore, Corporation Minière Golden Share / 2009 drilling program on the gold showing « RLM », Malartic Lake Shore property, Mining Corporation Golden Share. MERN report GM-64939.

Boyle, R.W. 1979. The geochemistry of gold and its deposits (together with a chapter on geochemical prospecting for the element). Geological Survey of Canada.

Bucholz, C.E., Jagoutz, O., Schmidt, M.W., and Sambuu, O. 2014. Fractional crystallization of high-K arc magmas: biotite-versus amphibole-dominated fractionation series in the Dariv Igneous complex, Western Mongolia. Contributions to Mineralogy and Petrology, **168**: 1072–1100.

Burrows, D.R., Spooner, E.T.C., Wood, P.C., and Jemielita, R.A. 1993. Structural controls on formation of the Hollinger-McIntyre Au quartz vein system in the Hollinger shear zone, Timmins, southern Abitibi greenstone belt, Ontario. Economic Geology, **88**: 1643–1663.

Camiré, G.E., Ludden, J.N., Flèche, M.R. La, and Burg, J.-P. 1993. Mafic and ultramafic amphibolites from the northwestern Pontiac subprovince: chemical characterization and implications for tectonic setting. Canadian Journal of Earth Sciences, **30**: 1110–1122.

Card, K.D. 1990. A review of the Superior Province of the Canadian Shield, a product of Archean accretion. Precambrian Research, **48**: 99–156.

655 Carter, M.W. 1992. Alkalic rocks of the Thunder Bay area. Ontario Geological Survey.
656 Chown, E.H., Daigneault, R., Mueller, W., and Mortensen, J.K. 1992. Tectonic evolution
657 of the northern volcanic zone, Abitibi belt, Quebec. Canadian Journal of Earth
658 Sciences, **29**: 2211–2225.
659 Corfu, F., Jackson, S.L., and Sutcliffe, R.H. 1991. U–Pb ages and tectonic significance of
660 late Archean alkalic magmatism and nonmarine sedimentation: Timiskaming Group,
661 southern Abitibi belt, Ontario. Canadian Journal of Earth Sciences, **28**: 489–503.
662 Côté-Vertefeuille, É. 2016. Caractérisation des dykes de lamprophyres en relation avec la
663 minéralisation aurifère de la Baie-James / Characterisation of lamprophyre dykes
664 related to gold mineralisation in the James Bay area. Unpublished B. Sc. honours
665 thesis GLG-3100, Laval University, Québec, Canada.
666 Currie, K.L., and Williams, P.R. 1993. An Archean calc-alkaline lamprophyre suite,
667 northeastern Yilgarn Block, western Australia. Lithos, **31**: 33–50.
668 Daigneault, R., Perreault, G., and Bedard, P. 1983. Geologie et geochimie de la mine
669 Lamaque, Val d'Or, Quebec. Canadian Institute of Mining and Metallurgical
670 Bulletin, **76**: 111–127.
671 Davis, D.W. 1998. Speculations on the formation and crustal structure of the Superior
672 Province from U-Pb geochronology. *In* Western Superior Transect Fourth Annual
673 Workshop. Lithoprobe Secretariat, University of British Columbia, Vancouver,
674 British Columbia, Lithoprobe Report No. 65. pp. 21–28.
675 Dubé, B., Williamson, K., McNicoll, V., Malo, M., Skulski, T., Twomey, T., and
676 Sanborn-Barrie, M. 2004. Timing of gold mineralization at Red Lake, Northwestern
677 Ontario, Canada: New constraints from U-Pb geochronology at the Goldcorp high-

678 grade zone, Red Lake mine, and the Madsen mine. Economic Geology, **99**: 1611–
679 1641.
680 Esperança, S., and Holloway, J.R. 1987. On the origin of some mica-lamprophyres:
681 experimental evidence from a mafic minette. Contributions to Mineralogy and
682 Petrology, **95**: 207–216.
683 Faure, S. 2015. Relations entre les minéralisations aurifères et les isogrades
684 métamorphiques en Abitibi / Relationship between gold mineralisations and
685 metamorphic isograde in Abitibi [online]. Consorem project 2013-03, available at:
686 http://www.consorem.ca/rapports_publics.html [cited in July 2017].
687 Gaulin, R., and Trudel, P. 1990. Caractéristiques pétrographiques et géochimiques de la
688 minéralisation aurifère à la mine Elder, Abitibi, Québec. Canadian Journal of Earth
689 Sciences, **27**: 1637–1650.
690 GEOROC. 2011. Geochemistry of Rocks of the Oceans and Continents [online]. Max-
691 Planck-Institut für Chemie, available at http://georoc.mpch-mainz.gwdg.de/georoc/
692 [cited in July 2017].
693 Gill, J., and Whelan, P. 1989. Early rifting of an oceanic island arc (Fiji) produced
694 shoshonitic to tholeiitic basalts. Journal of Geophysical Research: Solid Earth, **94**:
695 4561–4578.
696 Gill, R. 2010. Igneous rocks and processes: a practical guide. John Wiley & Sons.
697 Goldie, R. 1979. Consanguineous Archaean intrusive and extrusive rocks, Noranda,
698 Quebec: Chemical similarities and differences. Precambrian Research, **9**: 275–287.
699 Goutier, J., Gigon, J., Carl, G., François, H., Roman, H., Myriam, C.-R., Nathan, R.C.,
700 Adina, B., Antoine, R.O., and Fleury, J.-P. 2016. Les nouvelles interprétations

701 géologiques de la zone de contact entre les sous-provinces de La Grande et
702 d'Opinaca et leur importance pour l'exploration aurifère / New geological
703 interpretations of the contact between the La Grande and Opinaca subprovince.
704 MERN report DV 2016-03.
705 Goutier, J., and Melançon, M. 2010. Compilation géologique de la sous-province de
706 l'Abitibi (version préliminaire) / Geological compilation of the Abitibi subprovince
707 (preliminary). MERN report RP 2010-04.
708 Grant, M. 1986. Étude du métamorphisme et de la distribution verticale des teneurs en
709 Au, As et Sb à la mine Sigma, Val-d'Or, Québec / Study of metamorphism and
710 vertical distribution of Au, As and Sb grades at the Sigma mine, Val-d'Or, Québec.
711 Master thesis, École Polytechnique de Montréal, Québec, Canada.
712 Green, T.H., and Watson, E.B. 1982. Crystallization of apatite in natural magmas under
713 high pressure, hydrous conditions, with particular reference to "orogenic"rock
714 series. Contributions to Mineralogy and Petrology, **79**: 96–105.
715 Groves, D.I., Goldfarb, R.J., Gebre-Mariam, M., Hagemann, S.G., and Robert, F. 1998.
716 Orogenic gold deposits: a proposed classification in the context of their crustal
717 distribution and relationship to other gold deposit types. Ore geology reviews, **13**: 7–
718 27.
719 Guay, F., Pilote, P., and Daigneault, R. 2015. Minéralisation aurifère et déformation sur
720 l'indice Malartic Lakeshore, Sous-Province de l'Abitibi, Québec / Gold
721 mineralisation and deformation of the Malartic Lakeshore showing, Abitibi Sub-
722 Province, Québec. MERN report MB-2015-14.
723 Hattori, K., Hart, S.R., and Shimizu, N. 1996. Melt and source mantle compositions in

724 the Late Archaean: A study of strontium and neodymium isotope and trace elements
725 in clinopyroxenes from shoshonitic alkaline rocks. Geochimica et Cosmochimica
726 Acta, **60**: 4551–4562.
727 Hodgson, C.J., and Troop, D.G. 1988. A new computer-aided methodology for area
728 selection in gold exploration; a case study from the Abitibi greenstone belt.
729 Economic Geology, **83**: 952–977. Society of Economic Geologists.
730 Hofmann, A.W. 1988. Chemical differentiation of the Earth: the relationship between
731 mantle, continental crust, and oceanic crust. Earth and Planetary Science Letters, **90**:
732 297–314.
733 Jébrak, M., and Harnois, L. 1991. Two-stage evolution in an Archean tonalite suite: the
734 Taschereau stock, Abitibi (Quebec, Canada). Canadian Journal of Earth Sciences,
735 **28**: 172–183.
736 Jenney, C.P. 1961. Geology and ore deposits of the Mattagami area, Quebec. Economic
737 Geology, **56**: 740–757.
738 Jolly, W.T. 1974. Regional metamorphic zonation as an aid in study of Archean terrains:
739 Abitibi region, Ontario. Canadian Mineralogist, **12**: 499–508.
740 Kerrich, R. 1986. Fluid infiltration into fault zones: chemical, isotopic, and mechanical
741 effects. Pure and applied geophysics, **124**: 225–268.
742 Kerrich, R., and Wyman, D. 1990. Geodynamic setting of mesothermal gold deposits: An
743 association with accretionary tectonic regimes. Geology, **18**: 882–885.
744 Kerrich, R., and Wyman, D.A. 1994. The mesothermal gold-lamprophyre association:
745 significance for an accretionary geodynamic setting, supercontinent cycles, and
746 metallogenic processes. Mineralogy and Petrology, **51**: 147–172.

747 Kretschmar, U.H. 2011. Syngenetic gold: lode vein geology and exploration implications.
748 *In* World Gold 2011. Proceedings of the 50th Conference of Metallurgists. October
749 25. pp. 849–863.
750 Leake, B.E., Woolley, A.R., Arps, C.E.S., Birch, W.D., Gilbert, M.C., Grice, J.D.,
751 Hawthorne, F.C., Kato, A., Kisch, H.J., and Krivovichev, V.G. 1997. Report.
752 Nomenclature of Amphiboles: Report of the Subcommittee on Amphiboles of the
753 International Mineralogical Association Commission on New Minerals and Mineral
754 Names. Mineralogical magazine, **61**: 295–321.
755 Leduc, M. 1980. Géologie et lithogéochimie des masses batholitiques de la région de
756 Preissac / Geology and lithogeochemistry of batholites in the Preissac area. MERN
757 report DPV-779.
758 Lefèbvre, N., Kopylova, M., and Kivi, K. 2005. Archean calc-alkaline lamprophyres of
759 Wawa, Ontario, Canada: unconventional diamondiferous volcaniclastic rocks.
760 Precambrian Research, **138**: 57–87.
761 Lovell, H.L. 1972. Geology of Eby and Otto area, district of Timiskaming. *In* Geological
762 report 99. Ontario Department of Mines and Northern Affaires.
763 Le Maitre, R.W., Streckeisen, A., Zanettin, B., Le Bas, M.J., Bonin, B., Bateman, P.,
764 Bellieni, G., Dudek, A., Efremova, S., and Keller, J. 2002. Igneous rocks: A
765 classification and glossary of terms; Recommendations of the International Union of
766 Geological Sciences. *In* Subcommission on the Systematics of Igneous rocks.
767 Cambridge University Press. p. 230.
768 Mathieu, L. 2016. Quantifying hydrothermal alteration with normative minerals and other
769 chemical tools at the Beattie Syenite, Abitibi greenstone belt, Canada.

Geochemistry: Exploration, Environment, Analysis, **16**: 233–244. doi:10.1144/geochem2016-410.

McCulloch, M.T., and Gamble, J.A. 1991. Geochemical and geodynamical constraints on subduction zone magmatism. Earth and Planetary Science Letters, **102**: 358–374.

McNeil, A.M., and Kerrich, R. 1986. Archean lamprophyre dykes and gold mineralization, Matheson, Ontario: the conjunction of LILE-enriched mafic magmas, deep crustal structures, and Au concentration. Canadian Journal of Earth Sciences, **23**: 324–343.

Mitchell, R.H. 1994. The lamprophyre facies. Mineralogy and Petrology, **51**: 137–146.

Morin, D., Jébrak, M., Bardoux, M., and Goulet, N. 1993. Pontiac metavolcanic rocks within the Cadillac tectonic zone, McWatters, Abitibi belt, Quebec. Canadian Journal of Earth Sciences, **30**: 1521–1531.

Murphy, J.B. 2013. Appinite suites: a record of the role of water in the genesis, transport, emplacement and crystallization of magma. Earth-Science Reviews, **119**: 35–59.

Nadeau, O., Cayer, A., Pelletier, M., Stevenson, R., and Jébrak, M. 2015. The Paleoproterozoic Montviel carbonatite-hosted REE–Nb deposit, Abitibi, Canada: Geology, mineralogy, geochemistry and genesis. Ore Geology Reviews, **67**: 314–335.

Nadeau, O., Stevenson, R., and Jébrak, M. 2014. The Archean magmatic-hydrothermal system of Lac Shortt (Au-REE), Abitibi, Canada: insights from carbonate fingerprinting. Chemical Geology, **387**: 144–156.

Neumayr, P., Hagemann, S.G., and Couture, J.-F. 2000. Structural setting, textures, and timing of hydrothermal vein systems in the Val d'Or camp, Abitibi, Canada:

implications for the evolution of transcrustal, second-and third-order fault zones and gold mineralization. Canadian Journal of Earth Sciences, **37**: 95–114.

Owen, J.P. 2008. Geochemistry of lamprophyres from the Western Alps, Italy: implications for the origin of an enriched isotopic component in the Italian mantle. Contributions to Mineralogy and Petrology, **155**: 341–362.

Pearce, J.A. 1983. Role of the sub-continental lithosphere in magma genesis at active continental margins. *In* Continental basalts and mantle xenoliths, Nantwich, Cheshire. *Edited by* C.J. Hawkesworth and M.J. Norry. Shiva Publications. pp. 230–249.

Pearce, J.A. 2008. Geochemical fingerprinting of oceanic basalts with applications to ophiolite classification and the search for Archean oceanic crust. Lithos, **100**: 14–48.

Percival, J.A., Sanborn-Barrie, M., Skulski, T., Stott, G.M., Helmstaedt, H., and White, D.J. 2006. Tectonic evolution of the western Superior Province from NATMAP and Lithoprobe studies. Canadian Journal of Earth Sciences, **43**: 1085–1117. NRC Research Press.

Perring, C.S., Rock, N.M.S., Golding, S.D., and Roberts, D.E. 1989. Criteria for the recognition of metamorphosed or altered lamprophyres: a case study from the Archaean of Kambalda, Western Australia. Precambrian Research, **43**: 215–237.

Pilote, P. 2007. Géologie de la partie Ouest du Groupe de Malartic et corrélations à l'échelle de la Ceinture de l'Abitibi / Geology of the western part of Malartic Group and Abitibi greenstone belt-scale correlations. *In* Québec Exploration 2007. MERN file DV-2007-04. pp. 16–17.

Pilote, P. 2013. Géologie Malartic / Malartic geology. MERN map CG-32D01D-2013-

816 01.
817 Pilote, P. 2014. Architecture des Groupes de Malartic, de Piché et de Cadillac et de la
818 Faille de Cadillac, Abitibi - révision géologique, nouvelles datations et
819 interprétations / Architecture of the Malartic, Piché, and Cadillac Groups and of the
820 Cadillac fault zone, Abi. *In* Québec Mines 2014. MERN file DV-2015-03. p. 37.
821 Plá Cid, J., Nardi, L.V.S., Campos, C.S., Gisbert, P.E., Merlet, C., Conceição, H., and
822 Boyer, B. 2007. La, Ce, Nd, and Sr behavior in minette magmas during
823 crystallization of apatite-clinopyroxene-mica paragenesis at upper-mantle
824 conditions. European Journal of Mineralogy, **19**: 39–50.
825 Robert, F., and Brown, A.C. 1986. Archean gold-bearing quartz veins at the Sigma Mine,
826 Abitibi greenstone belt, Quebec; Part I, Geologic relations and formation of the vein
827 system. Economic Geology, **81**: 578–592.
828 Rock, N.M.S. 1987. The nature and origin of lamprophyres: an overview. Geological
829 Society, London, Special Publications, **30**: 191–226.
830 Rock, N.M.S. 1991. Nature, Origin and Evolution of Lamprophyre Melts. *In*
831 Lamprophyres. Springer. pp. 125–149.
832 Rock, N.M.S., and Groves, D.I. 1988a. Can lamprophyres resolve the genetic controversy
833 over mesothermal gold deposits? Geology, **16**: 538–541.
834 Rock, N.M.S., and Groves, D.I. 1988b. Do lamprophyres carry gold as well as diamonds?
835 Nature, **332**: 235–255. doi:10.1038/332253a0.
836 Ropchan, J.R., Luinstra, B., Fowler, A.D., Benn, K., Ayer, J., Berger, B., Dahn, R.,
837 Labine, R., and Amelin, Y. 2002. Host-rock and structural controls on the nature and
838 timing of gold mineralization at the Holloway Mine, Abitibi Subprovince, Ontario.

839 Economic Geology, **97**: 291–309.
840 Rowins, S.M., Cameron, E.M., Lalonde, A.E., and Ernst, R.E. 1993. Petrogenesis of the
841 late Archean syenitic Murdock Creek pluton, Kirkland Lake, Ontario: Evidence for
842 an extensional tectonic setting. Canadian Mineralogist, **31**: 219.
843 Rowins, S.M., Lalonde, A.E., and Cameron, E.M. 1991. Magmatic oxidation in the
844 syenitic Murdock Creek intrusion, Kirkland Lake, Ontario: evidence from the
845 ferromagnesian silicates. The Journal of Geology, **99**: 395–414.
846 Sarbas, B., and Nohl, U. 2008. The GEOROC database as part of a growing
847 geoinformatics network [online]. *In* Geoinformatics conference. GSA. Available
848 from https://gsa.confex.com/gsa/2008GE/finalprogram/abstract_142093.htm
849 [accessed in July 2017].
850 Schandl, E.S., O'Hanley, D.S., and Wicks, F.J. 1989. Rodingites in serpentinized
851 ultramafic rocks of the Abitibi greenstone belt, Ontario. The Canadian Mineralogist,
852 **27**: 579–591.
853 Schulz, K.J., Smith, I.E.M., and Blanchard, D.P. 1979. The nature of Archean alkalic
854 rocks from the southern portion of the Superior Province. Eos, **60**: 410.
855 Scott, C.R., Mueller, W.U., and Pilote, P. 2002. Physical volcanology, stratigraphy, and
856 lithogeochemistry of an Archean volcanic arc: evolution from plume-related
857 volcanism to arc rifting of SE Abitibi Greenstone Belt, Val d'Or, Canada.
858 Precambrian Research, **115**: 223–260.
859 Sims, P.K., and Mudrey, J.M.G. 1972. Syenitic plutons and associated lamprophyres. *In*
860 Geology of Minnesota: a centennial volume. *Edited by* P.K. Sims and G.B. Morey.
861 Minnesota Geological Survey, Minneapolis. pp. 140–152.

862 Sparks, R.S.J., Pinkerton, H., and Macdonald, R. 1977. The transport of xenoliths in
863 magmas. Earth and Planetary Science Letters, **35**: 234–238.
864 Spera, F.J. 1984. Carbon dioxide in petrogenesis III: role of volatiles in the ascent of
865 alkaline magma with special reference to xenolith-bearing mafic lavas.
866 Contributions to Mineralogy and Petrology, **88**: 217–232.
867 Streckeisen, A. 1979. Classification and nomenclature of volcanic rocks, lamprophyres,
868 carbonatites, and melilitic rocks: Recommendations and suggestions of the IUGS
869 Subcommission on the Systematics of Igneous Rocks. Geology, **7**: 331–335.
870 Sutcliffe, R.H., Barrie, C.T., Burrows, D.R., and Beakhouse, G.P. 1993. Plutonism in the
871 southern Abitibi Subprovince; a tectonic and petrogenetic framework. Economic
872 Geology, **88**: 1359–1375. SecG.
873 Sutcliffe, R.H., Smith, A.R., Doherty, W., and Barnett, R.L. 1990. Mantle derivation of
874 Archean amphibole-bearing granitoid and associated mafic rocks: evidence from the
875 southern Superior Province, Canada. Contributions to Mineralogy and Petrology,
876 **105**: 255–274.
877 Taner, M.F., and Chemam, M. 2015. Algoma-type banded iron formation (BIF), Abitibi
878 Greenstone belt, Quebec, Canada. Ore Geology Reviews, **70**: 31–46.
879 Taner, M.F., and Trudel, P. 1991. Gold distribution in the Val-d'Or Formation and a
880 model for the formation of the Lamaque–Sigma mines, Val-d'Or, Quebec. Canadian
881 Journal of Earth Sciences, **28**: 706–720.
882 Thompson, J.E., and Griffis, A.T. 1941. Geology of Gauthier Township, east Kirkland
883 Lake area. Ontario Department of Mines Annual Report.
884 Thompson, R.N., Morrison, M.A., Dickin, A.P., and Hendry, G.L. 1983. Continental

885 flood basalts... Arachnids rule OK? *In* Continental basalts and mantle xenoliths,
886 Nantwich, Cheshire. *Edited by* C.J. Hawkesworth and M.J. Norry. Shiva
887 Publications. pp. 158–185.
888 Thompson, R.N., Morrison, M.A., Hendry, G.L., Parry, S.J., Simpson, P.R., Hutchison,
889 R., and O'Hara, M.J. 1984. An Assessment of the Relative Roles of Crust and
890 Mantle in Magma Genesis: An Elemental Approach [and Discussion]. Philosophical
891 Transactions of the Royal Society of London A: Mathematical, Physical and
892 Engineering Sciences, **310**: 549–590.
893 Thurston, P.C., Ayer, J.A., Goutier, J., and Hamilton, M.A. 2008. Depositional gaps in
894 Abitibi greenstone belt stratigraphy: A key to exploration for syngenetic
895 mineralization. Economic Geology, **103**: 1097–1134.
896 Ubide, T., Galé, C., Arranz, E., Lago, M., and Larrea, P. 2014. Clinopyroxene and
897 amphibole crystal populations in a lamprophyre sill from the Catalonian Coastal
898 Ranges (NE Spain): a record of magma history and a window to mineral-melt
899 partitioning. Lithos, **184**: 225–242.
900 Venturelli, G., Thorpe, R.S., Dal Piaz, G. V, Del Moro, A., and Potts, P.J. 1984.
901 Petrogenesis of calc-alkaline, shoshonitic and associated ultrapotassic Oligocene
902 volcanic rocks from the northwestern Alps, Italy. Contributions to Mineralogy and
903 Petrology, **86**: 209–220.
904 Watson, K.D. 1957. Hornblende lamprophyre dykes in southwestern Lesueur Township,
905 Quebec. Canadian Mineralogist, **6**: 15–30.
906 Wesley McCall, G., Nabelek, P.I., Bauer, R.L., and Glascock, M.D. 1990. Petrogenesis
907 of Archean lamprophyres in the southern Vermilion Granitic Complex, northeastern

Minnesota, with implications for the nature of their mantle source. Contributions to Mineralogy and Petrology, **104**: 439–452.

Williams, F. 2002. Diamonds in Late Archean calc–alkaline lamprophyres Ontario, Canada: origins and implications. Unpublished B. Sc. honours thesis, University of Sydney, Sydney, Australia,.

Wilson, H.S. 1936. The geology of Lamaque Mine. Canadian Mining Journal, **57**: 511–516.

Wyman, D.A., Ayer, J.A., Conceição, R. V, and Sage, R.P. 2006. Mantle processes in an Archean orogen: evidence from 2.67 Ga diamond-bearing lamprophyres and xenoliths. Lithos, **89**: 300–328.

Wyman, D.A., and Kerrich, R. 1988. Archean lamprophyres, gold deposits and transcrustal structures: Implications for greenstone belt gold metallogeny. Economic Geology, **93**: 454–459.

Wyman, D.A., and Kerrich, R. 1993. Archean shoshonitic lamprophyres of the Abitibi Subprovince, Canada: petrogenesis, age, and tectonic setting. Journal of Petrology, **34**: 1067–1109.

Wyman, D.A., Kerrich, R., and Polat, A. 2002. Assembly of Archean cratonic mantle lithosphere and crust: plume–arc interaction in the Abitibi–Wawa subduction–accretion complex. Precambrian Research, **115**: 37–62.

Wyman, D., and Kerrich, R. 1989a. Archean shoshonitic lamprophyres associated with Superior Province gold deposits: distribution, tectonic setting, noble metal abundances, and significance for gold mineralization. Economic Geology Monograph, **6**: 651–667.

931 Wyman, D., and Kerrich, R. 1989b. Archean lamprophyre dikes of the Superior Province,
932 Canada: distribution, petrology, and geochemical characteristics. Journal of
933 Geophysical Research: Solid Earth, **94**: 4667–4696.
934 Wyman, D., and Kerrich, R. 2009. Plume and arc magmatism in the Abitibi subprovince:
935 implications for the origin of Archean continental lithospheric mantle. Precambrian
936 Research, **168**: 4–22.
937 Wyman, D., and Kerrich, R. 2010. Mantle plume–volcanic arc interaction: consequences
938 for magmatism, metallogeny, and cratonization in the Abitibi and Wawa
939 subprovinces, Canada This article is one of a series of papers published in this
940 Special Issue on the theme Lithoprobe—parameters, pr. Canadian Journal of Earth
941 Sciences, **47**: 565–589.
942 Wyman, D., Kerrich, R., and Sun, M. 1995. Noble metal abundances of late Archean (2.7
943 Ga) accretion-related shoshonitic lamprophyres, Superior Province, Canada.
944 Geochimica et cosmochimica acta, **59**: 47–57.
945 Yoder, H.S., and Tilley, C.E. 1962. Origin of basalt magmas: an experimental study of
946 natural and synthetic rock systems. Journal of Petrology, **3**: 342–532.
947 Zhang, J., Lin, S., Linnen, R., and Martin, R. 2014. Structural setting of the Young-
948 Davidson syenite-hosted gold deposit in the western Cadillac-Larder Lake
949 deformation zone, Abitibi greenstone belt, Superior Province, Ontario. Precambrian
950 Research, **248**: 39–59.
951
952

Table captions

Table 1: Identification criteria for lamprophyres

Table 2: Chemical analyses of the studied samples

Table 3: Results (eigenvalues) of PCA

Table 4: Approximate proportions (vol%) of phases observed in thin sections

Table 5: Texture of amphibole and biotite

Table 6: General formula of the analysed amphiboles based on 23 oxygens (Lamp_FG samples)

Table 7: Identification criteria for lamprophyres applied to the studied samples

Figure captions

Figure 1: Location of the CAL intrusions considered by this study. The geological map is from the MERN (SIGEOM; http://sigeom.mines.gouv.qc.ca) and OGS (http://www.geologyontario.mndm.gov.on.ca) and the projection is UTM NAD83 zone 17. The « other rocks » category corresponds to the gneiss of the SIGEOM map; i.e. rocks metamorphosed to the upper Amphibolite or Granulite facies. Red and white dots locate the studied samples, and red dots locate the CAL observed by various authors in the Abitibi Subprovince (Thompson and Griffis 1941, Watson 1957, Jenney 1961, Lovell 1972, Goldie 1979, McNeil and Kerrich 1986, Schandl et al. 1989, Barrie 1990, Gaulin and Trudel 1990, Sutcliffe et al. 1990, Jébrak and Harnois 1991, Barrie and Shirey 1991, Rowins et al. 1991, 1993, Bourne and Bossé 1991, Corfu et al. 1991, Bédard and Chown

975 1992, Chown et al. 1992, Morin et al. 1993, Burrows et al. 1993, Camiré et al. 1993,
976 Barber 1996, Hattori et al. 1996, Bleeker and Parrish 1996, Neumayr et al. 2000,
977 Ropchan et al. 2002, Kretschmar 2011, Nadeau et al. 2014, 2015, Zhang et al. 2014,
978 Taner and Chemam 2015).

979 **Figure 2:** Field pictures of the Lamp_FG dykes (a) and of the xenolith-bearing
980 Lamp_AL intrusion (b). The pen used as scale is 14.5 cm long.

981 **Figure 3:** Total Alkali Silicate diagram (TAS diagram; Le Bas et al. 1992) showing the
982 variable chemical composition of calc-alkaline (CAL), alkaline (AL), and ultramafic
983 (UM) lamprophyres (after Rock 1987, as reported by Gill 2010). The studied samples are
984 reported, as well as chemical compositions of CAL compiled from the literature (see text
985 for references).

986 **Figure 4:** Arachnid diagrams showing: a) the immobile trace elements-content of the
987 studied and compiled CAL (elements order is from Pearce 2008), as well as the mean La
988 content of basalt, andesite, dacite and rhyolite compiled from he Georoc database, and of
989 the cumulate, diorite, and syenite units of the Murdock Creek intrusion (Rowins et al.
990 1993); and b) the median composition of samples from the Georoc and Beakhouse (2011)
991 databases, distributed between categories A (for trachyte, trachyandesite, and the « other
992 » group; see text for details on each category), B (minor, minor intrusion, syntectonic), C
993 (lamprophyres), and D (other compiled categories; see text for details).

994 **Figure 5:** Results of PCA shown as a binary diagram of the first and second principal
995 components (PC1 and PC2). The Pie diagrams display the simplified names of the
996 samples located in and outside of the circled area. The studied samples, the abitibian
997 CAL compiled from the literature (labelled « Lamprophyre compiled »), and the analyses

998 from the Georoc dataset and from Beakhouse (2011) (labelled « Other rocks ») are
999 displayed.

1000 **Figure 6:** Pictures of the Lamp_BJ (a to d) and Lamp_Carb (e, f) samples observed in
1001 natural (a to e) and polarised (f) lights. The abbreviations are Act (actinolite), Hbl
1002 (hornblende), Bt (biotite), Fsp (feldspar), Cb (carbonate), and Chl (chlorite).

1003 **Figure 7:** Samples FG-07 (a, b), FG-02 (c, d), and Lamp_AL (e, f) observed in natural
1004 light (a, c, e), as well as interpreted and simplified mineralogy as observed in thin
1005 sections (b, d, f). The main minerals observed in samples FG-07, FG-02, and Lamp_AL,
1006 respectively, are represented in red for amphibole (56, 15, and 21 vol% in the displayed
1007 image), green for biotite and chlorite (6, 32, and 28 vol%), white for feldspar and quartz
1008 (33, 38, and 48 vol%), and black for epidote (5, 16, and 2 vol%).

1009 **Figure 8:** Backscattered electron SEM images of sample FG-07 and sketch (b). The
1010 abbreviations used are A, B, and C (for zones A, B, and C amphiboles), Ep (epidote), Bt
1011 (biotite), and Fsp (feldspar).

1012 **Figure 9:** Backscattered electron SEM images of sample FG-07, draped with chemical
1013 maps of major elements (a, b). Note the biotite inclusions (yellow) observed in zone B
1014 amphibole (a, b). An intensely altered part of the sample is also displayed (c) and the
1015 mineralogy of this area is interpreted (d) using the following colors: red for amphibole
1016 (Amp), black for feldspar (Fsp), green for biotite (Bt), white for epidote (Ep), yellow for
1017 calcite (Cal), and purple for titanite (Ttn) and ±apatite.

1018 **Figure 10:** Backscattered electron SEM images of sample FG-02 (a, c) draped with
1019 interpreted mineralogy (b, d) and chemical maps of major elements (e, f). The following
1020 colors are used (b, d): red for amphibole, black for feldspar, green for biotite and

1021 ±chlorite, white for epidote, and purple for titanite and ±apatite. The abbreviations used
1022 are: Amp (amphibole), Ep (epidote), Bt (biotite), Chl (chlorite), Qz (quartz), and Fsp
1023 (feldspar).

1024 **Figure 11:** Chemical compositions of the amphiboles of samples FG-07 (a) and FG-02
1025 (b) represented using the Leake et al. (1997) diagram for Ca-amphiboles characterised by
1026 $(Na+K)_A < 0.5$. The empty symbols correspond to Ca-amphiboles characterised by
1027 $(Na+K)_A \geq 0.5$ that should be displayed on another diagram. Note that the analysis of a
1028 Ca-Na amphibole (magnesiokatophorite; sample FG-02) is not represented.

1029 **Figure 12:** Chemical composition of biotites from the Lamp_FG samples.

1030 **Figure 13:** Arachnid diagram showing the immobile trace elements-content of the
1031 Lamp_AL samples (elements order is from Pearce 2008). The "diorite" samples come
1032 from diorite and quartz diorite rocks of the "main chimney" plug (Lamaque mine) studied
1033 by Daigneault et al. (1983).

1034 **Figure 14:** Compilation of mafic lamprophyres observed in the Abitibi Subprovince
1035 (Québec). The geological map is from the MERN (SIGEOM;
1036 http://sigeom.mines.gouv.qc.ca), the projection is UTM NAD83 zone 17, and the color
1037 code is the same as in Figure 1. Red/orange and white dots locate the studied samples,
1038 red/orange dots locate the CAL referred to by various authors in the Abitibi Subprovince
1039 (see Figure 1 for references), and black/purple dots locate the mafic lamprophyres
1040 observed or compiled by the MERN.

1041

Tables

Table 1: Identification criteria for lamprophyres

Criterion	Description
	Field
Ia	Small-volume intrusions
Ib	Biotite and/or amphibole macrocrysts
Ic	Xenolith, ocelli
	Chemistry
IIa	Mantle-derived mafic magma
IIb	Enriched source
IIc	Small degree partial melting
IId	Relative depletion in HFSE
	Petrology
IIIa	Magmatic CO_2- and H_2O-bearing phases
IIIb	Unusual crystallisation sequence
IIIc	Amphibole chemistry
IIId	Biotite chemistry

Table 2: Chemical analyses of the studied samples

	Lamp_AL							Lamp_FG		Lamp_Carb	Lamp_BJ			
Sample	64870	64869	64868	64855	64865	64866	64856	FG-07	FG-02	ML-05-056	98-FF-11108-A1	99-JG-1200-B	99-MH-4589	11-JG-1197-A
Latitude	48.1034	48.1034	48.1030	48.1022	48.1016	48.1016	48.1022	48.2314	48.2315	48.1917	53.4146	53.7940	53.8179	53.5226
Longitude	-77.7232	-77.7232	-77.7237	-77.7238	-77.7238	-77.7238	-77.7238	-78.1519	-78.1521	-79.4686	-77.3635	-76.8201	-76.5334	-74.1560
SiO_2 (wt%)	57.31	57.13	53.73	48.63	51.84	50.92	48.95	57.44	56.68	43.36	51.00	55.40	52.70	53.09
TiO_2	0.51	0.60	0.66	0.81	0.66	0.71	0.81	0.53	0.76	0.76	0.33	0.57	0.73	0.57
Al_2O_3	14.16	14.80	13.71	12.64	12.87	13.24	14.12	13.84	15.64	10.68	9.43	12.70	14.40	12.87
$Fe_2O_3^T$	6.41	7.30	8.30	8.76	9.22	9.38	10.37	6.19	8.47	8.24	8.43	8.25	8.99	8.45
CaO	5.07	6.10	7.73	9.59	8.25	8.25	8.96	7.24	6.53	10.59	6.84	6.87	7.81	7.52
MgO	5.07	6.08	7.37	13.27	9.15	9.59	9.23	5.45	4.25	5.81	17.30	7.53	7.38	10.69
MnO	0.11	0.13	0.15	0.25	0.16	0.17	0.23	0.14	0.13	0.15	0.15	0.13	0.14	0.14
K_2O	2.33	2.83	2.20	1.20	2.70	2.56	0.78	0.61	1.90	2.34	0.08	1.73	2.46	1.57
Na_2O	3.78	3.03	3.37	1.56	2.37	2.56	2.39	5.77	4.47	1.06	0.96	4.16	3.55	2.96
P_2O_5	0.29	0.34	0.38	0.41	0.38	0.37	0.38	0.27	0.32	0.45	0.19	0.29	0.32	0.23
LOI	4.48	2.12	2.66	3.23	2.12	1.98	2.89	1.72	1.39	16.30	4.28	1.34	0.89	1.40
Total	99.52	100.46	100.26	100.35	99.72	99.73	99.10	99.20	100.54	99.74	98.99	98.97	99.37	99.49
Mg#[a]	0.61	0.62	0.64	0.75	0.66	0.67	0.64	0.64	0.50	0.58	0.80	0.64	0.62	0.71
Eu (ppm)	1.32	1.47	1.55	1.42	1.35	1.36	1.59	1.37	1.65	1.89	0.60	1.14	1.42	0.95
Lu	0.25	0.28	0.29	0.29	0.27	0.29	0.31	0.13	0.27	0.37	0.14	0.17	0.19	0.18
Th	4.73	4.66	4.18	2.78	3.02	3.06	3.62	3.42	4.21	4.40	2.72	3.23	2.79	2.80
Nb	4.80	5.30	4.90	3.40	3.90	3.90	4.60	5.60	4.30	5.90	2.70	5.40	3.30	3.90
Ta	0.40	0.43	0.34	0.28	0.28	0.32	0.35	0.26	0.39	0.30	0.22	0.27	0.20	0.30
La	29.10	30.60	28.70	18.60	20.60	20.50	24.90	33.00	25.60	36.40	13.40	19.80	21.60	10.80
Ce	59.50	64.30	62.10	42.20	44.40	45.30	54.80	67.20	55.10	82.50	25.90	46.80	47.60	34.20
Pr	6.80	7.57	7.49	5.44	5.52	5.70	6.77	8.72	6.99	9.66	3.19	6.13	6.24	3.62
Nd	26.50	29.20	30.10	23.70	22.60	23.40	28.50	34.10	29.00	38.70	11.70	25.40	26.90	15.00
Zr	120	122	103	90	96	93	104	117	139	121	67	87	89	77

Hf	2.60	2.50	2.40	2.10	2.80	2.10	2.30	3.20	3.40	4.00	1.70	2.40	2.30	1.80
Sm	5.18	5.71	6.16	5.23	4.96	5.18	5.94	5.51	6.04	7.60	2.28	4.26	5.11	3.07
Gd	4.07	4.71	4.91	4.67	4.28	4.38	5.18	3.66	4.86	6.07	1.68	3.35	3.69	2.68
Tb	0.57	0.63	0.66	0.64	0.58	0.59	0.69	0.41	0.64	0.82	0.26	0.45	0.51	0.42
Dy	3.15	3.33	3.54	3.56	3.12	3.40	3.66	2.00	3.59	4.78	1.56	2.32	2.62	2.19
Ho	0.57	0.62	0.67	0.70	0.59	0.66	0.71	0.00	0.00	0.91	0.29	0.46	0.52	0.45
Y	16.00	18.30	19.50	19.40	17.40	19.00	20.00	10.00	18.50	26.80	8.60	12.30	13.90	11.70
Er	1.65	1.78	1.91	1.95	1.73	1.92	2.02	0.94	1.96	2.57	0.89	1.27	1.48	1.28
Tm	0.25	0.26	0.28	0.29	0.25	0.27	0.30	0.14	0.29	0.38	0.13	0.19	0.22	0.18
Yb	1.60	1.73	1.86	1.87	1.60	1.95	1.95	0.85	1.86	2.31	0.83	1.18	1.32	1.19
Cr	242	290	368	667	459	465	414	534	82	274	1860	396	338	
Co	23	27	34	55	38	39	42	25	23	28	51	27	29	38
Ni	78	91	110	354	168	175	133	85	31	52	570	79	44	118
La/Y	1.82	1.67	1.47	0.96	1.18	1.08	1.25	3.3	1.38	1.36	1.56	1.61	1.55	0.92

6 [a]Mg# = MgO/(MgO+FeO^T) (molar)

Table 3: Results (eigenvalues) of PCA

	PC1	PC2	PC3
Th_ABS	0.336	-0.793	-0.088
Yb_ABS	0.286	0.507	-0.641
ZrHf_Ano	-0.864	-0.047	-0.033
Slope	0.242	0.333	0.762
Variance explained	40.1%	19.7%	10%

Table 4: Approximate proportions (vol%) of phases observed in thin sections

Sample	Sample #	Amp[a]	Bt[b]	Fsp[c]	Quartz	Epidote	Opaque	Carbonate
Lamp_Carb	ML-05-056		20	15	25		10	30
Lamp_FG	FG-02	15	20	40	10	12	<3	2
	FG-07	38	5	48		5	3	0 to 10[d]
Lamp_AL	Lamp_AL	20	25	40	0 to 10	<5		<5
Lamp_BJ	98-FF-11108-A1	70		20			5	5
	99-JG-1200-B	35	15	45	5		<3	
	99-MH-4589	30	25	40	5		<3	
	11-JG-1197-A	40	25	35			<3	

[a]Amp – amphibole, mostly hornblende and actinolite

[b]Bt – biotite, poorly to abundantly replaced by retrograde chlorite

[c]Fsp – feldspars, mostly albite and ±microcline

[d]Carbonate – enriched patches, only observed in the central part of the dyke

17 **Table 5:** Texture of amphibole and biotite

Sample	Textures
Lamp_Carb	• Amphibole pseudomorphed by chlorite-carbonate-quartz assemblages; • Alteration-related carbonate-filled vesicles.
Lamp_FG	• Brown (sample 11-JG-1197-A) or green (other samples) hornblende; • Hornblende resorbed by the feldspar-dominated matrix (sample 99-JG-1200-B); • Xenomorphic biotite growing at the expense of amphibole and defining the main foliation plane (sample 11-JG-1197-A mostly); • Amphibole containing euhedral elongated biotite oblique to the main foliation plane; • Clusters of amphibole and biotite megacrysts (sample 99-MH-4589).
Lamp_AL	• Biotite macrocrysts partially retrograded to chlorite; • Biotite growing at the expense of amphibole.
Lamp_BJ	• Zoned euhedral amphiboles (FG-07); • Alignment of amphiboles corresponding to a magmatic flowage organisation (FG-07); • Un-zoned amphibole resorbed by matrix minerals (feldspar ±quartz) (FG-02); • Biotite partially retrograded to chlorite; • Coarse biotite that forms elongated clusters (FG-07); • Biotite growing at the expense of amphibole.

18

19

Table 6: General formula of the analysed amphiboles based on 23 oxygens (Lamp_FG samples)

	FG-07						FG-02			
	Zone A (n=17)		Zone B (n=13)		Zone C (n=23)		Zone B (n=5)		Zone C (n=19)	
	Med[a]	St.d.	Med	St.d.	Med	St.d.	Med	St.d.	Med	St.d.
Si (T[b])	6.54	0.08	6.40	0.15	7.63	0.17	6.35	0.13	7.76	0.15
Ti	0.15	0.02	0.14	0.04	0	0.005	0.17	0.04	0	0.02
Al (T)	1.46	0.08	1.60	0.15	0.37	0.18	1.65	0.13	0.24	0.15
Al (C)	0.31	0.11	0.35	0.05	0.12	0.08	0.32	0.04	0.04	0.28
Fe^{3+} (C)	0.56	0.17	0.67	0.17	0.23	0.12	0.59	0.12	0.18	0.09
Mg (C)	2.91	0.52	2.41	0.17	3.55	0.22	2.39	0.10	3.68	0.28
Fe^{2+} (C)	1.09	0.55	1.41	0.20	1.05	0.11	1.54	0.17	1.02	0.06
Fe^{2+} (B)	0	0	0	0	0	0.01	0	0	0	0.10
Mn (C)	0.04	0.02	0.04	0.01	0.02	0.02	0.05	0.01	0.03	0.02
Mn (B)	0	0	0	0	0.003	0.01	0	0	0.01	0.01
Ca (B)	1.80	0.04	1.87	0.02	1.94	0.04	1.82	0.07	1.96	0.24
Na (B)	0.20	0.04	0.13	0.02	0.05	0.04	0.18	0.07	0.03	0.14
Na (A)	0.26	0.05	0.28	0.04	0.06	0.04	0.28	0.07	0.02	0.03
K (A)	0.15	0.01	0.15	0.02	0	0.02	0.20	0.03	0	0.15

[a]Med, median, and St.d., standard deviation.

[b]A, B, C and T refer to the crystallographic sites in the standard amphibole formula $AB_2{}^{VI}C_5{}^{IV}T_8O_{22}(OH)_2$ (Leake et al. 1997).

Table 7: Identification criteria for lamprophyres applied to the studied samples

	Lamp_Carb	Lamp_FG		Lamp_AL	Lamp_BJ			
Criterion	**ML-05-056**	**FG-02**	**FG-07**	**Lamp_AL**	**98-FF-11108-A1**	**99-JG-1200-B**	**99-MH-4589**	**11-JG-1197-A**
Ia	possibly	✓	✓	✓	✓	✓	✓	✓
Ib	possibly	✓	✓	✓	✓	✓	✓	✓
Ic		NO	NO	xenolith	NO	NO	xenolith?	NO
IIa	✓	✓	✓	✓	✓	✓	✓	✓
IIb	✓	✓	✓	✓	±	✓	✓	±
IIc				unconclusive				
IId	✓	✓	✓	✓	NO	✓	✓	✓
IIIa			✓					
IIIb			✓					
IIIc		±	✓					
IIId								

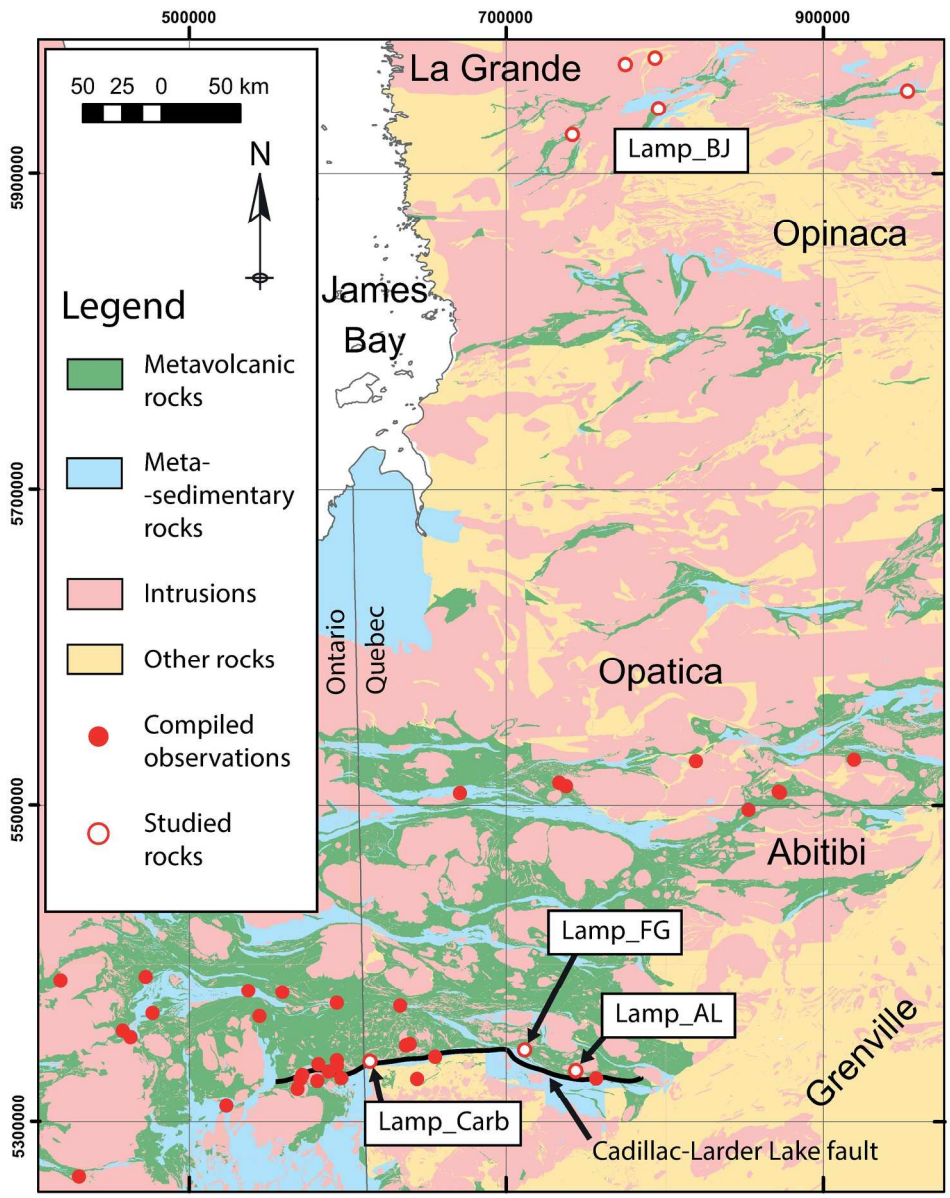

Location of the CAL intrusions considered by this study. The geological map is from the MERN (SIGEOM; http://sigeom.mines.gouv.qc.ca) and OGS (http://www.geologyontario.mndm.gov.on.ca) and the projection is UTM NAD83 zone 17. The « other rocks » category corresponds to the gneiss of the SIGEOM map; i.e. rocks metamorphosed to the upper Amphibolite or Granulite facies. Red and white dots locate the studied samples, and red dots locate the CAL observed by various authors in the Abitibi Subprovince (Thompson and Griffis 1941, Watson 1957, Jenney 1961, Lovell 1972, Goldie 1979, McNeil and Kerrich 1986, Schandl et al. 1989, Barrie 1990, Gaulin and Trudel 1990, Sutcliffe et al. 1990, Jébrak and Harnois 1991, Barrie and Shirey 1991, Rowins et al. 1991, 1993, Bourne and Bossé 1991, Corfu et al. 1991, Bédard and Chown 1992, Chown et al. 1992, Morin et al. 1993, Burrows et al. 1993, Camiré et al. 1993, Barber 1996, Hattori et al. 1996, Bleeker and Parrish 1996, Neumayr et al. 2000, Ropchan et al. 2002, Kretschmar 2011, Nadeau et al. 2014, 2015, Zhang et al. 2014, Taner and Chemam 2015).

185x232mm (300 x 300 DPI)

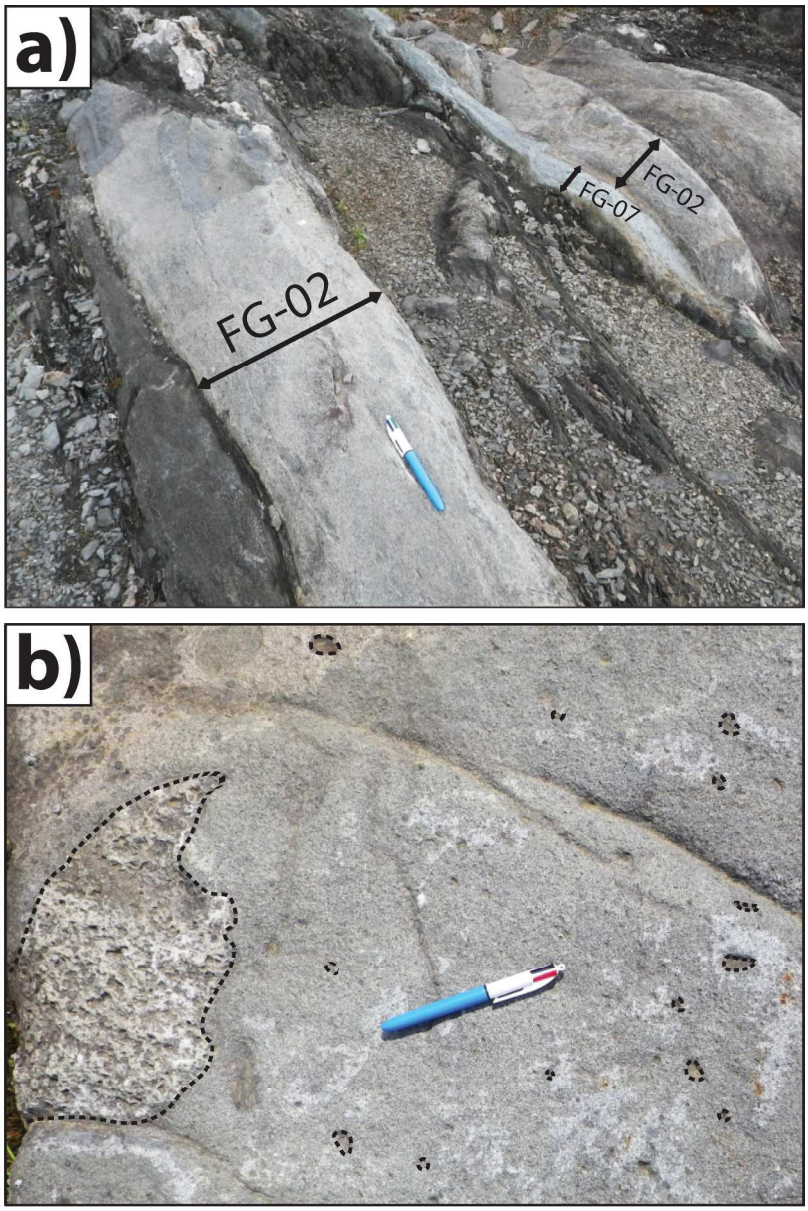

Figure 2: Field pictures of the Lamp_FG dykes (a) and of the xenolith-bearing Lamp_AL intrusion (b). The pen used as scale is 14.5 cm long.

183x272mm (300 x 300 DPI)

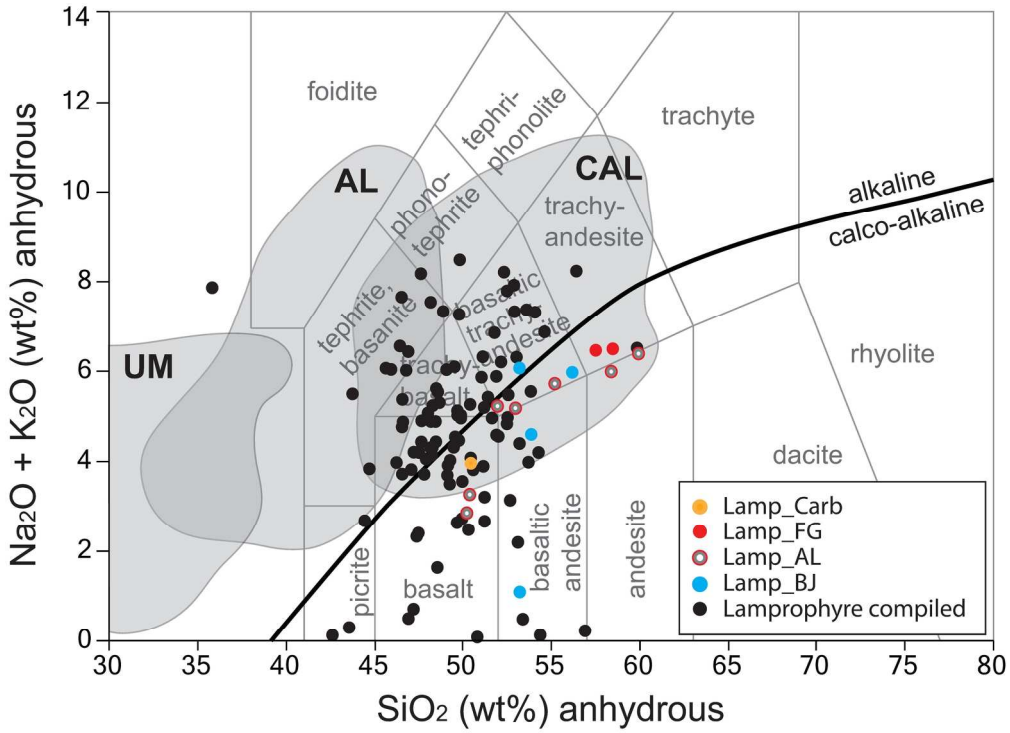

Figure 3: Total Alkali Silicate diagram (TAS diagram; Le Bas et al. 1992) showing the variable chemical composition of calc-alkaline (CAL), alkaline (AL), and ultramafic (UM) lamprophyres (after Rock 1987, as reported by Gill 2010). The studied samples are reported, as well as chemical compositions of Abitibian CAL compiled from the literature (see text for references).

185x135mm (300 x 300 DPI)

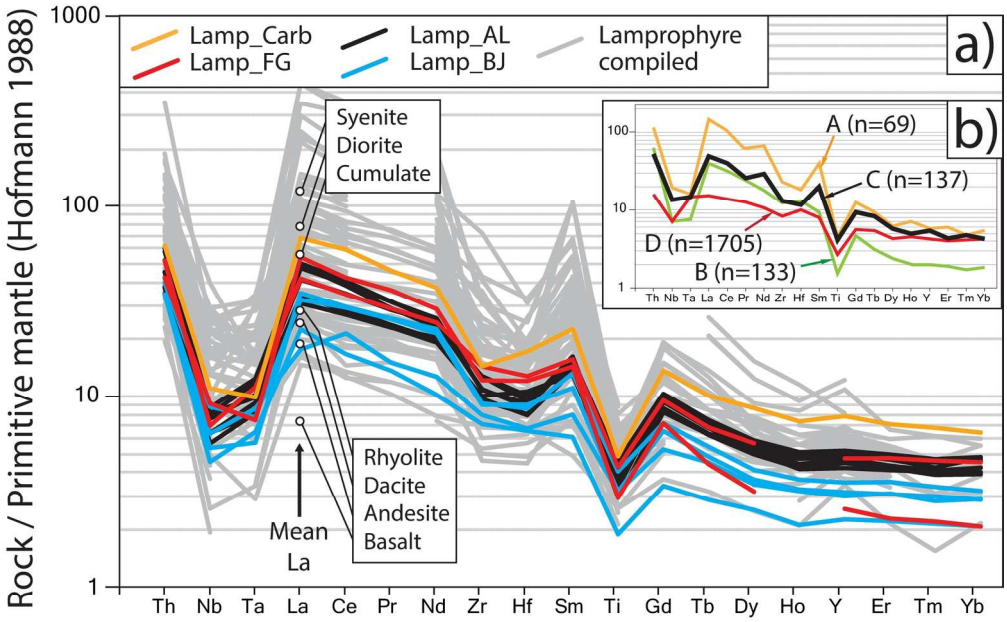

Arachnid diagrams showing: a) the immobile trace elements-content of the studied and compiled CAL (elements order is from Pearce 2008), as well as the mean La content of basalt, andesite, dacite and rhyolite compiled from he Georoc database, and of the cumulate, diorite, and syenite units of the Murdock Creek intrusion (Rowins et al. 1993); and b) the median composition of samples from the Georoc and Beakhouse (2011) databases, distributed between categories A (for trachyte, trachyandesite, and the « other » groups; see text for details on each category), B (minor, minor intrusion, syntectonic), C (lamprophyres), and D (all the other categories compiled; see text for details).

171x118mm (300 x 300 DPI)

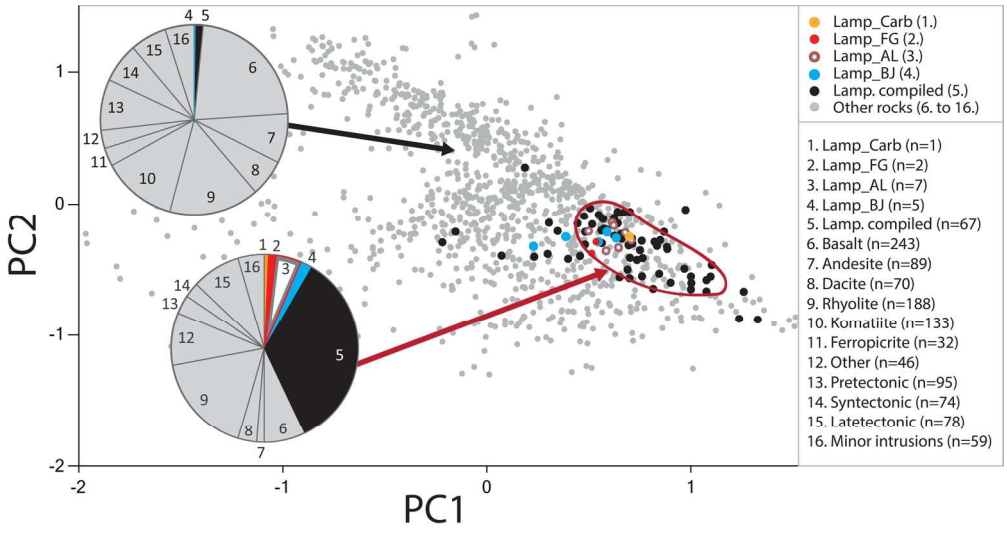

Results of PCA shown as a binary diagram of the first and second principal components (PC1 and PC2). The Pie diagrams display the simplified names of the samples located in and outside of the circled area. The studied samples, the abitibian CAL compiled from the literature (labelled « Lamprophyre compiled »), and the analyses from the Georoc dataset and from Beakhouse (2011) (labelled « Other rocks ») are displayed.

169x89mm (300 x 300 DPI)

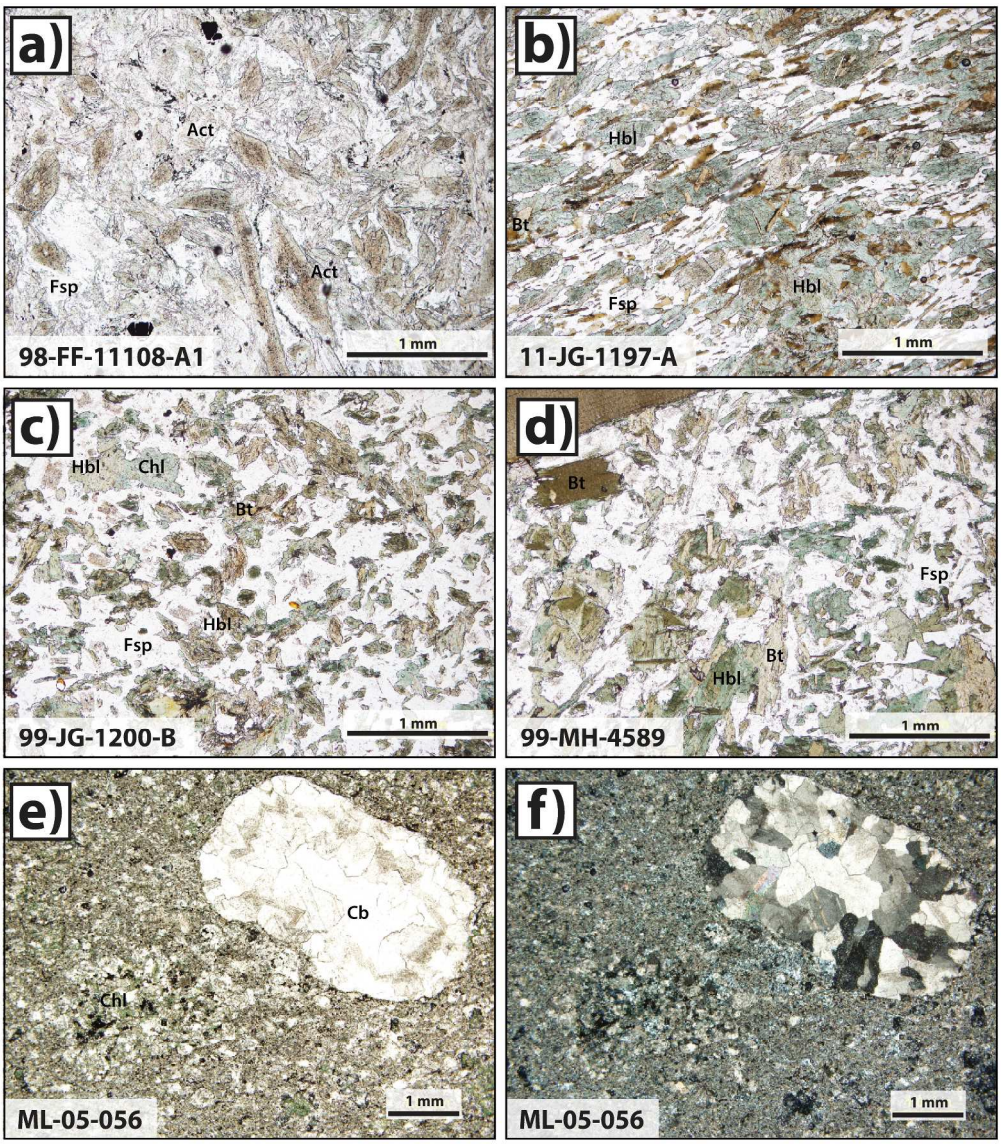

Figure 6: Pictures of the Lamp_BJ (a to d) and Lamp_Carb (e, f) samples observed in natural (a to e) and polarised (f) lights. The abbreviations are Act (actinolite), Hbl (hornblende), Bt (biotite), Fsp (feldspar), Cb (carbonate), and Chl (chlorite).

254x289mm (300 x 300 DPI)

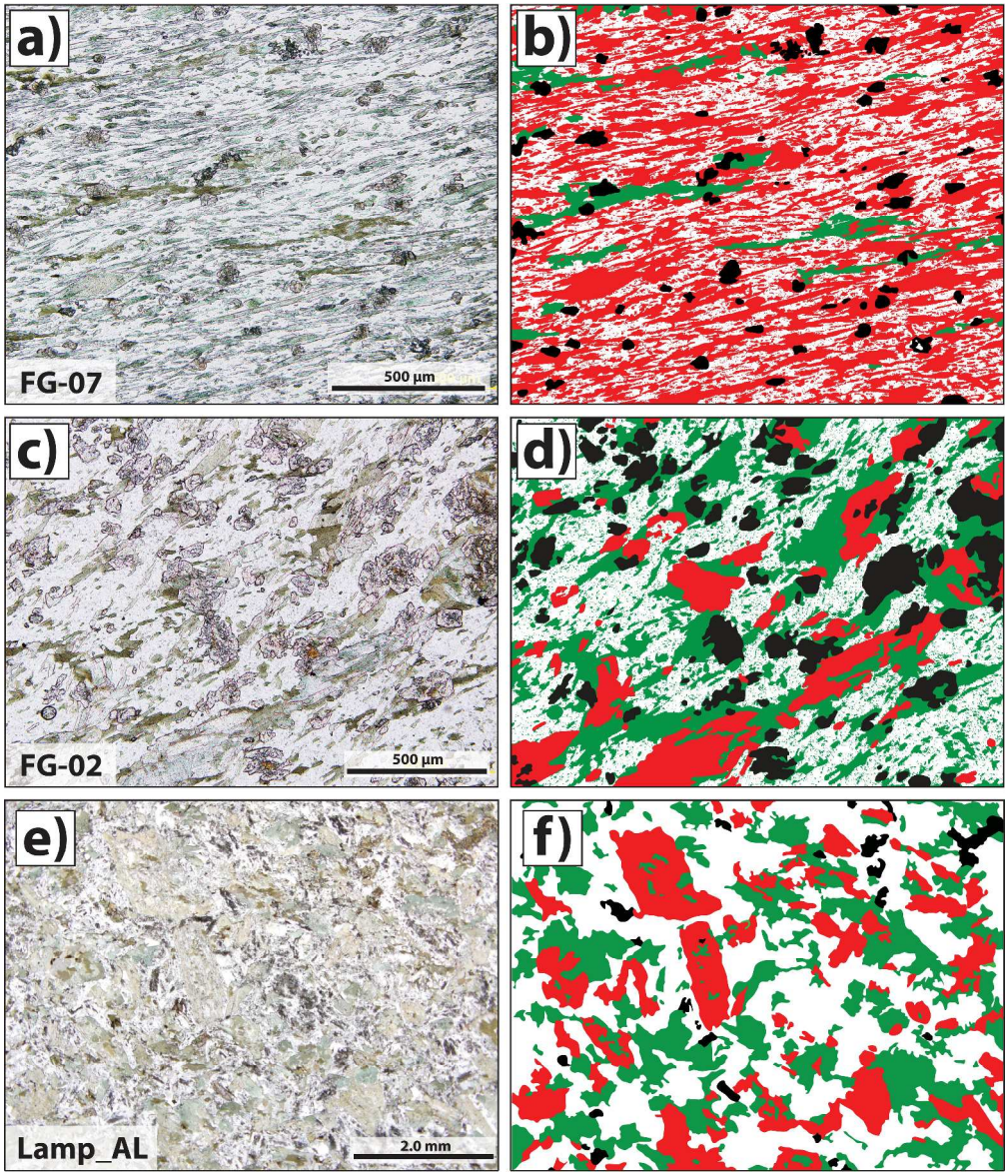

Figure 7: Samples FG-07 (a, b), FG-02 (c, d), and Lamp_AL (e, f) observed in natural light (a, c, e), as well as interpreted and simplified mineralogy as observed in thin section (b, d, f). The main minerals observed in samples FG-07, FG-02, and Lamp_AL, respectively, are represented in red for amphibole (56, 15, and 21 vol% in the displayed image), green for biotite and chlorite (6, 32, and 28 vol%), white for feldspar and quartz (33, 38, and 48 vol%), and black for epidote (5, 16, and 2 vol%).

485x567mm (600 x 600 DPI)

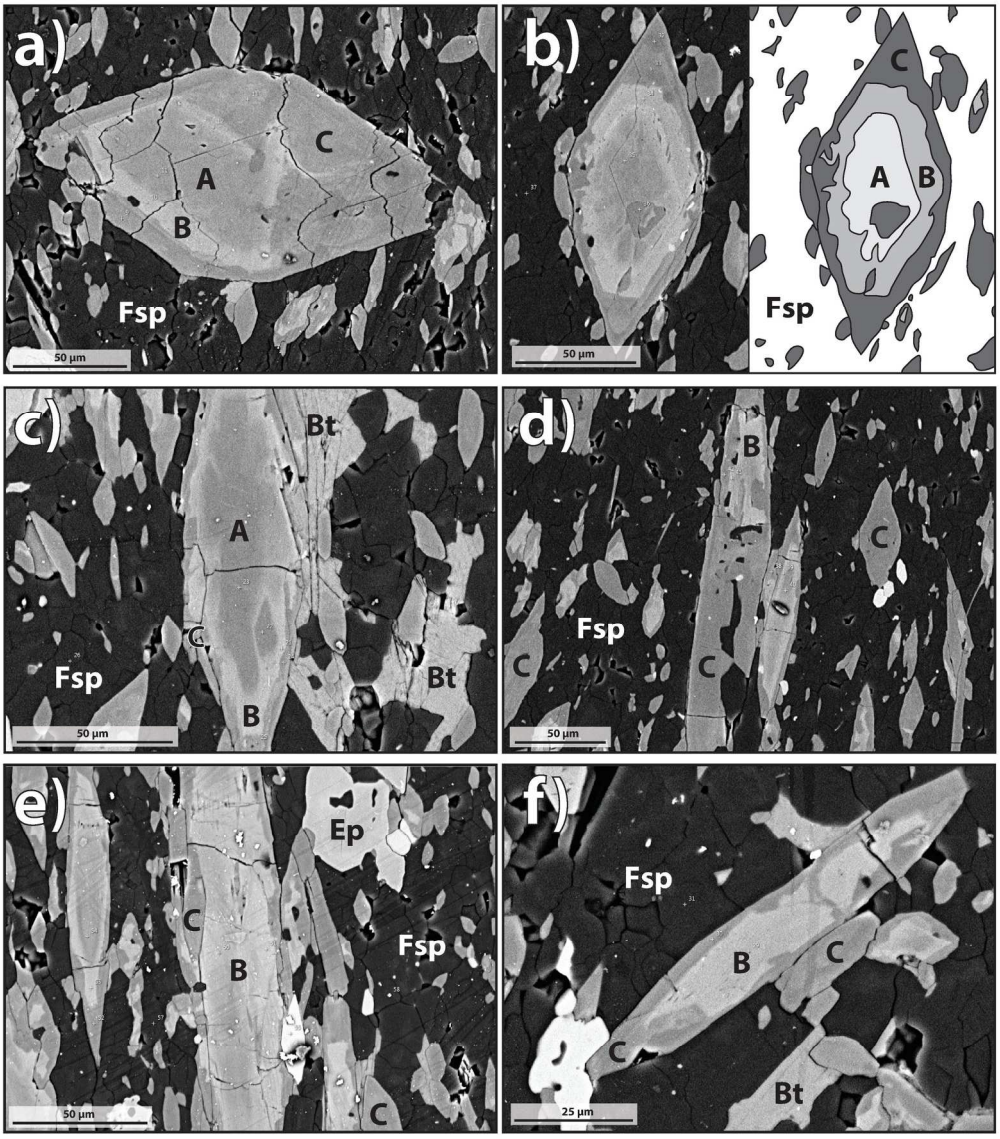

Figure 8: Backscattered electron SEM images of sample FG-07 and sketch (b). The abbreviations used are A, B, and C (for zones A, B, and C amphiboles), Ep (epidote), Bt (biotite), and Fsp (feldspar).

182x211mm (300 x 300 DPI)

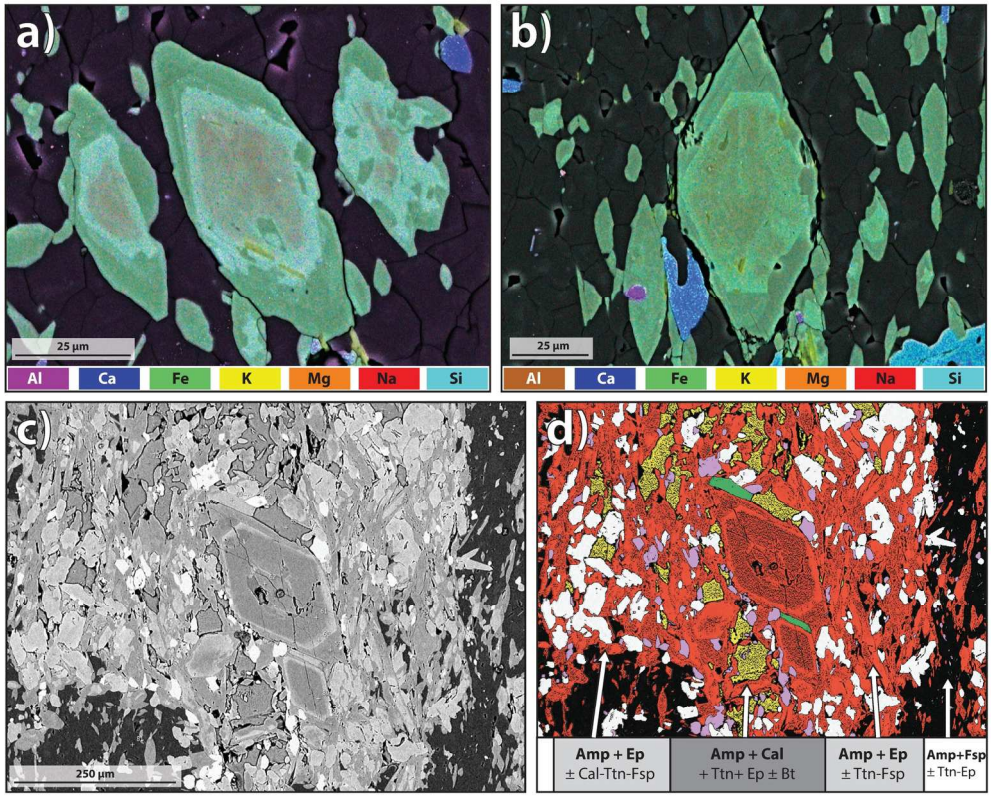

Figure 9: Backscattered electron SEM images of sample FG-07, draped with chemical maps of major elements (a, b). Note the biotite inclusions (yellow) observed in zone B amphibole (a, b). An intensely altered part of the sample is also displayed (c) and the mineralogy of this area is interpreted (d) using the following colors: red for amphibole (Amp), black for feldspar (Fsp), green for biotite (Bt), white for epidote (Ep), yellow for calcite (Cal), and purple for titanite (Ttn) and ±apatite.

176x144mm (300 x 300 DPI)

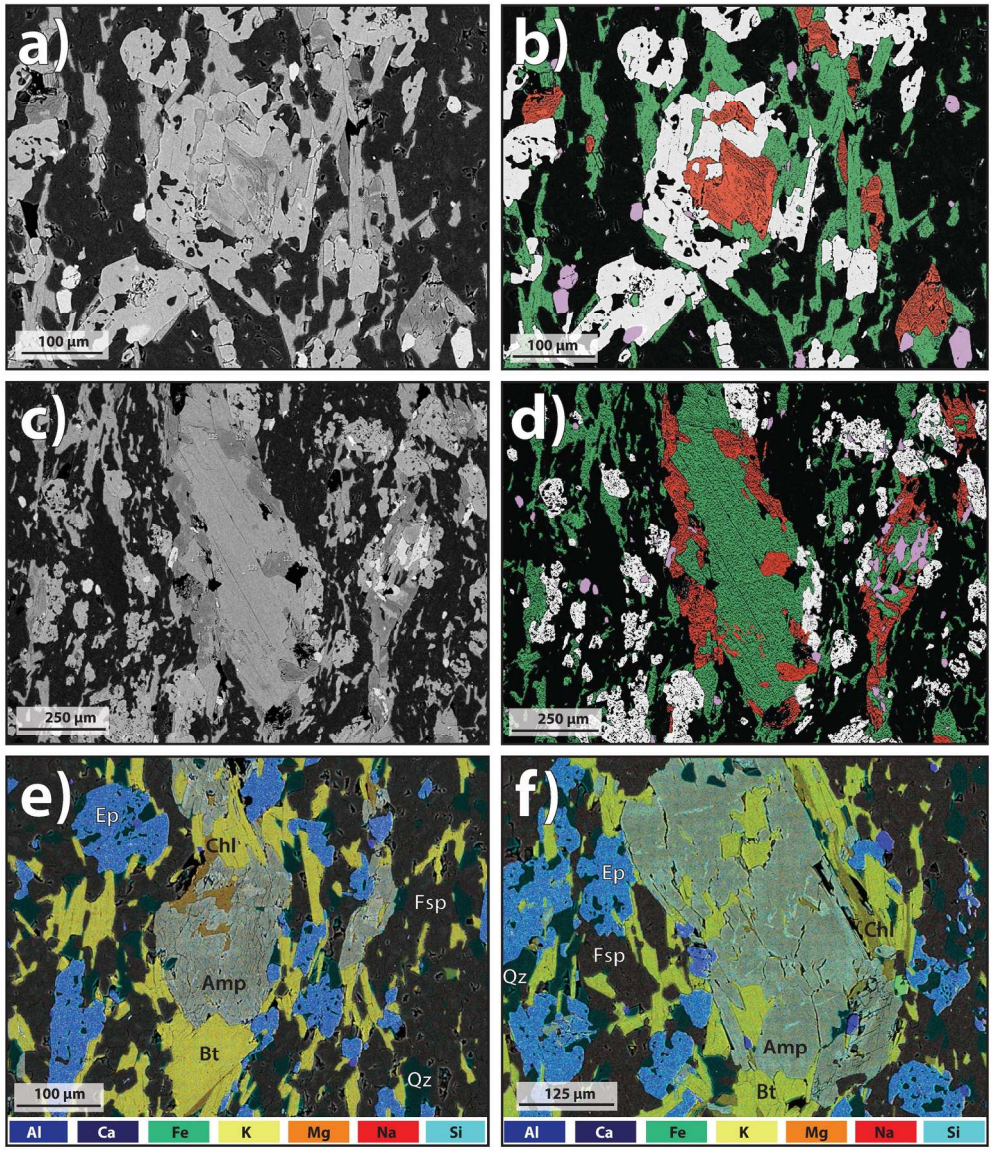

Figure 10: Backscattered electron SEM images of sample FG-02 (a, c) draped with interpreted mineralogy (b, d) and chemical maps of major elements (e, f). The following colors are used (b, d): red for amphibole, black for feldspar, green for biotite and ±chlorite, white for epidote, and purple for titanite and ±apatite. The abbreviations used are: Amp (amphibole), Ep (epidote), Bt (biotite), Chl (chlorite), Qz (quartz), and Fsp (feldspar).

187x217mm (300 x 300 DPI)

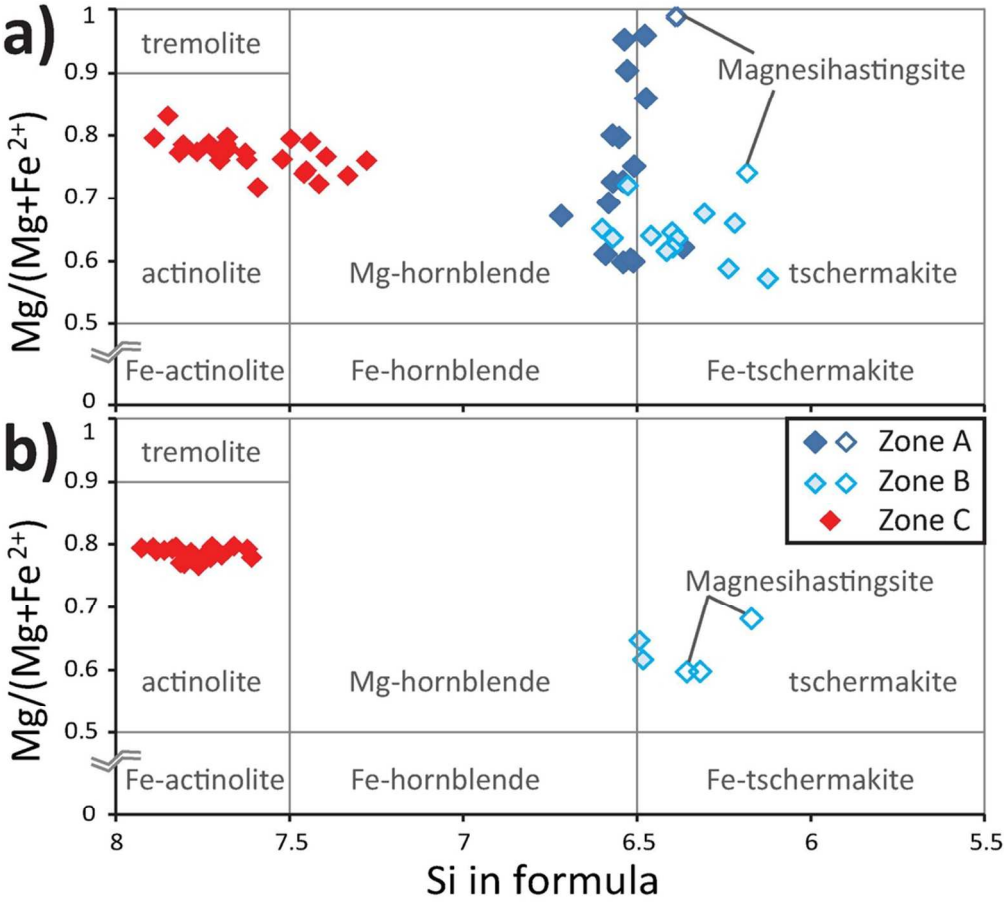

Figure 11: Chemical compositions of the amphiboles of samples FG-07 (a) and FG-02 (b) represented using the Leake et al. (1997) diagram for Ca-amphiboles characterised by (Na+K)A < 0.5. The empty symbols correspond to Ca-amphiboles characterised by (Na+K)A ≥ 0.5 that should be displayed on another diagram. Note that the analysis of a Ca-Na amphibole (magnesiokatophorite; sample FG-02) is not represented.

88x80mm (300 x 300 DPI)

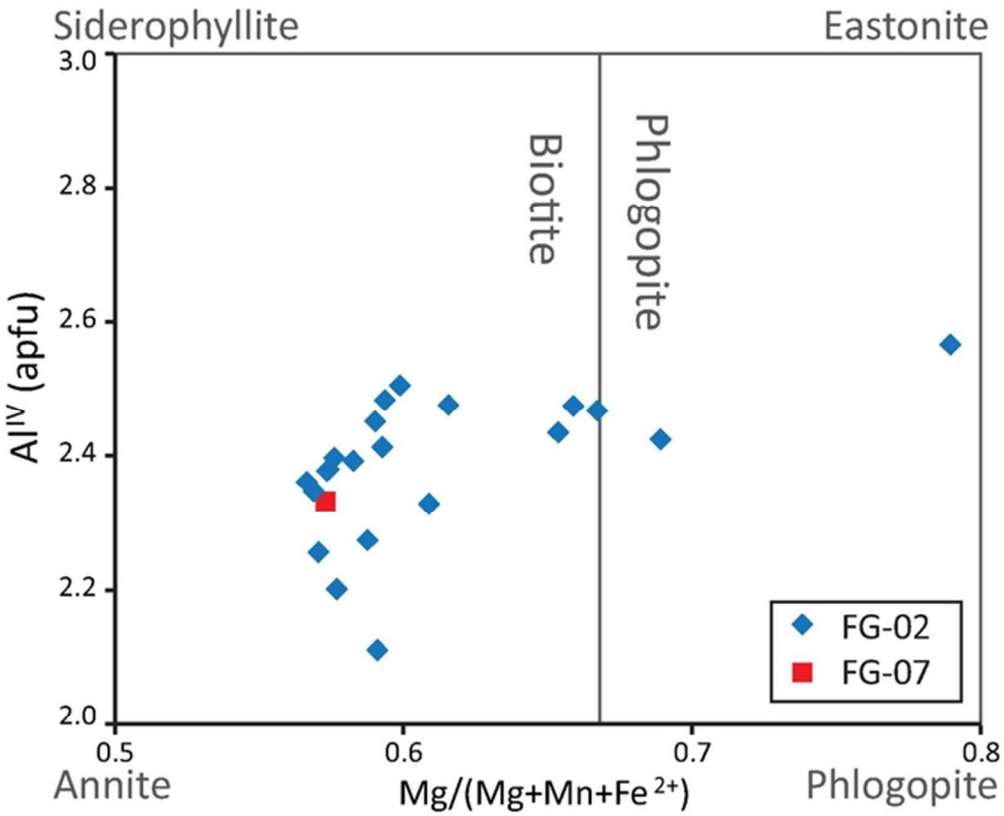

Figure 12: Chemical composition of biotites from the Lamp_FG samples.

56x46mm (300 x 300 DPI)

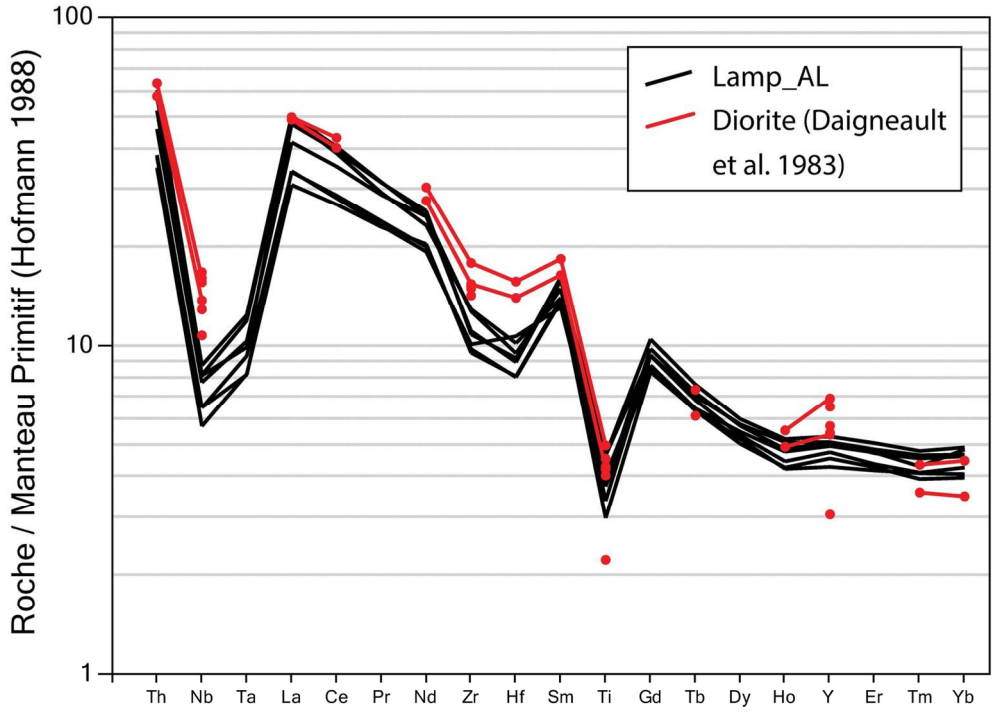

Figure 13: Arachnid diagram showing the immobile trace elements-content of the Lamp_AL samples (elements order is from Pearce 2008). The "diorite" samples come from diorite and quartz diorite rocks of the "main chimney" plug (Lamaque mine) studied by Daigneault et al. (1983).

139x98mm (300 x 300 DPI)

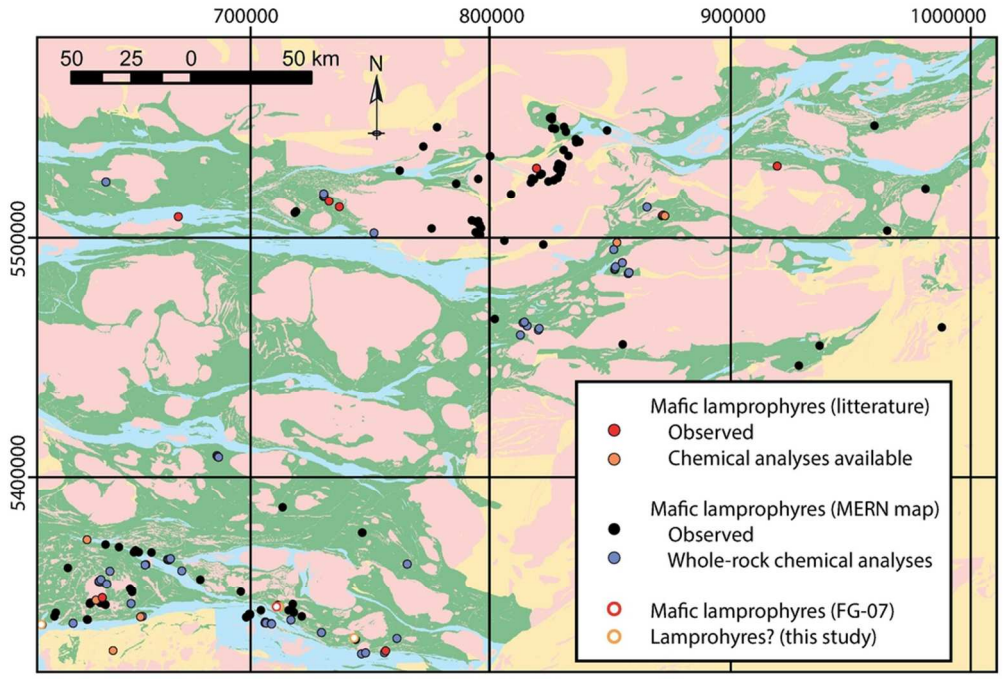

Compilation of mafic lamprophyres observed in the Abitibi Subprovince (Québec). The geological map is from the MERN (SIGEOM; http://sigeom.mines.gouv.qc.ca), the projection is UTM NAD83 zone 17, and the color code is the same as in Figure 1. Red/orange and white dots locate the studied samples, red/orange dots locate the CAL referred to by various authors in the Abitibi Subprovince (see Figure 1 for references), and black/purple dots locate the mafic lamprophyres observed or compiled by the MERN.

90x61mm (300 x 300 DPI)